The effective interaction between nucleons deduced from nuclear spectra*

John P. Schiffer

Argonne National Laboratory, Argonne, Illinois 60439
and University of Chicago, Chicago, Illinois 60637

William W. True

University of California, Davis, California 95616

Two-body matrix elements of the residual nucleon–nucleon interaction are extracted from experimental data throughout the periodic table and are used to determine the ranges and well depths of various components of a local interaction. The $T = 1$ even and odd components of the central interaction both definitely require two wells with different ranges; a shorter-range attractive well with a longer-range repulsive one. The need for a tensor interaction and a two-body spin–orbit interaction is also explored and their inclusion improves the fit slightly.

CONTENTS

*Work performed under the auspices of the U. S. Energy Research and Development Administration.

I. INTRODUCTION

Practically all microscopic calculations in nuclear structure use a "residual" or "effective" two-body interaction between valence nucleons. Because one has a many-body problem that cannot be treated exactly, the residual interaction between valence nucleons used in most calculations is not the same interaction as the one obtained from fitting the experimental data of two freely interacting nucleons (Bohr and Mottelson, 1969).

The many-body aspect of the problem forces several restrictions and approximations on any practical calculation of nuclear structure. All systems have an infinite number of degrees of freedom and one usually expresses this fact by using an appropriate infinite set of basis states; in practice these must be truncated to a finite set. This truncation is usually performed so as to retain those states which are expected to play the most important role in describing the nuclear energy levels being studied. The extent of the truncation is also governed by the size and speed of the computers used in the calculations. In addition, the Hamiltonian of the system is usually approximated by replacing the sum of the two-body interactions between all the nucleons by a common single-particle potential (which includes a spin–orbit term) and a two-body residual interaction acting between the "active valence nucleons."

The introduction of this single-particle potential into the Hamiltonian and, more importantly, the truncation of the infinite set of basis states causes the effective nucleon–nucleon interaction to be changed from the free-nucleon case. There are several approaches which are usually used. One approach is to try and take into account the effect of truncation by using the reaction matrix approach (Kuo and Brown, 1966; 1968; Kuo, 1974; Macfarlane, 1969; Lawson, 1971; Herling and Kuo, 1972; McGrory *et al.*, 1970; Ko *et al.*, 1973). Typical calculations using this approach have been done by Kuo and Brown (see above references). Another approach is to use a phenomenological force for the residual interaction between nucleons. Typical calculations using this approach have been done by Kim and Rasmussen (1963, 1964), Harvey and Clement (1971), Vary and Ginocchio (1971), and Ma and True (1973). Both approaches have their "good points" and their "bad points" and use several parameters which are adjusted to give the best fit to

the experimental data. The reaction matrix approach is basically more appealing in that it is on firmer theoretical grounds. However, calculating the matrix elements using the reaction matrix approach is more difficult and the matrix elements are usually evaluated by taking the first few terms in an infinite series. It is not clear at this point whether important contributions to these matrix elements have been neglected because not enough terms in the infinite series were retained (Osnes and Warke, 1969; Barrett and Kirson, 1970; Goode, 1974; Goode and Koltun, 1972; Barrett, 1975). A third approach, that is applicable in a few restricted regions of the periodic table, is to do a least-squares fit to a selected set of experimental data, which are assumed to belong within one configuration. Usually the data fitted consists of the energies of the nuclear states, with the matrix elements of the residual interaction treated as free parameters which are varied to give best fit. Once such matrix elements are determined, the resultant wave functions can be checked for "further" consistency by seeing how well they describe other nuclear phenomena such as moments, and electromagnetic and beta-decay transition rates. Alternatively, if one determines the matrix elements for two particles in a given j shell, they can be used with fractional parentage coefficients to predict the matrix elements for n particles in that shell. Typical calculations, utilizing these methods have been done by Meshkov and Ufford (1956), by Talmi and collaborators (Talmi and Thieberger, 1956; Goldstein and Talmi, 1957; and Talmi, 1957), by Cohen and Kurath (1965), by Cohen *et al.* (1967), and by Arima *et al.* (1968).

In selected nuclei throughout the periodic table, it is possible to determine reasonably well from experimental data the value of the diagonal matrix elements of the residual interaction, generally by relying on transfer reactions to determine the excitation energies, angular momenta, parities, configurations, and admixtures of relevant states.

For example, consider the ^{209}Bi$(d,p)^{210}$Bi reaction. Since the ^{209}Bi ground state is essentially a $1h_{9/2}$ proton outside the ^{208}Pb core,[1] the (d,p) reaction with angular momentum transfer j is expected to populate strongly those levels in ^{210}Bi which have a $|1h_{9/2}jJ\rangle$ configuration. Here $|jj'J\rangle$ represents a particle with an angular momentum j vector coupled to another particle with j', to form total angular momentum J.

Using the binding energies of ^{209}Bi, ^{209}Pb, and ^{210}Bi relative to ^{208}Pb, and the single-neutron excitation energies for orbits with angular momentum j in ^{209}Pb, it is possible to calculate the excitation energy E_0 at which the multiplet $|1h_{9/2}j\rangle$ would appear, in the absence of a residual interaction, in ^{210}Bi:

$$\begin{aligned} E_0(h_{9/2},j) &\equiv \{B[^{209}\mathrm{Bi}] - B[^{208}\mathrm{Pb}]\} + \{B[^{209}\mathrm{Pb}^*(j)] - B[^{208}\mathrm{Pb}]\} \\ &\quad - \{B[^{210}\mathrm{Bi}] - B[^{208}\mathrm{Pb}]\} \\ &= B[^{209}\mathrm{Bi}] + B[^{209}\mathrm{Pb}^*(j)] - B[^{210}\mathrm{Bi}] - B[^{208}\mathrm{Pb}] \,. \end{aligned} \tag{I.1}$$

[1]To the extent that the ^{209}Bi ground state and ^{209}Pb single-particle states involve "core polarization," in some sense, it is the residual interaction of nucleons in these "clothed" single-particle states that one extracts from the data.

$B[\,]$ is the total binding energy of the particular nucleus described in the bracket. The two-body residual interaction removes the degeneracy of the multiplet that would have been expected at excitation energy E_0. The actual excitation energies of the levels E_J^* then depend on J and, provided that one has a pure configuration, the difference $E_J = E_J^* - E_0$ is a measure of the two-body matrix element. This procedure makes sense if the states in ^{210}Bi can indeed be identified with the pure $|1h_{9/2}jJ\rangle$ configuration.

In a few cases, as will be discussed in Sec. II, a given $|jj'J\rangle$ configuration is distributed among two or more actual levels.[2] However, with sufficient experimental data, it is possible to deduce the energy centroid of the unperturbed two-particle configuration and thus one is still able to determine the value of the two-body matrix element.

A particle missing from an otherwise filled shell (i.e., $2j$ particles in a shell j) may be regarded as a "hole." Two holes or a hole and a particle with respect to a closed core can also be used to determine two-body matrix elements. Two holes can be treated in exactly the same manner as two particles and the matrix elements can be determined directly from the experimental data. If one knows the matrix elements of a given hole–particle configuration, $|j_1^{-1}j_2J\rangle$, it is possible to convert the hole–particle matrix elements into the particle–particle matrix elements by using the relation

$$E_J^{(p-p)}(j_1j_2) = -\sum_{J'}[J']W(j_1j_2j_2j_1;JJ')E_{J'}^{(p-h)}(j_1j_2), \tag{I.2}$$

where $E_J(j_1j_2) \equiv \langle j_1j_2J|V|j_1j_2J\rangle$, $W(abcd;ef)$ is the Racah coefficient, and $[J']$ is used to denote $(2J'+1)$. Equation (I.2) is often called the "Pandya transformation" (Pandya, 1956; Goldstein and Talmi, 1956). For a more general treatment of spectroscopic relationships see Koltun (1973).

This method of determining the two-body diagonal matrix element from the experimental data works well provided that the states are quite pure with little or no configuration mixing, or that the fragmentation is known and the centroids are used.

Data collected in this way have been analyzed in earlier papers. In Moinester *et al.* (1969), data then available, mostly of the mixed isospin n–p type, were tabulated and similarities were noted in the corresponding multipole coefficients. All the n–p data were fitted quite well by a delta-function force with an exchange mixture; the agreement was not so good for the $j_1 = j_2$ data. The

[2]The test for such admixtures is in the cross section to members of the multiplet. For the example of ^{209}Bi$(d,p)^{210}$Bi, each member of the $\pi 1h_{9/2}\nu 2g_{9/2}$ multiplet should have $(2J+1)/(2j_2+1)(2j_1+1)$ times the cross section of the ^{208}Pb$(d,p)^{209}$Pb reaction to the $2g_{9/2}$ ground state of ^{209}Pb (except for small corrections due to kinematics). If there is some admixing with other states, then this cross section will be further fragmented in proportion to such admixtures. If the spins and the transferred l and j values are known, then the unperturbed energies may be computed. The cross sections thus give a reliable test of the purity of a two-nucleon multiplet relative to the adjacent single-nucleon state.

interpretation was carried somewhat further by Schiffer (1971 a and 1971 b). When more data became available for multiplets in different isospin states, the data were reanalyzed in terms of different components of a central interaction (Schiffer, 1972; Anantaraman and Schiffer, 1972). Since that time additional data have been collected and the present work is a systematic reanalysis of the data available by approximately mid 1975. A slightly earlier version of these results appears in Schiffer, 1975.

Unfortunately, there are not enough reliable experimental data available at the present time to determine the off-diagonal elements from the transfer reactions. If enough data were available to treat these more complex cases, one would then be able to also determine off-diagonal matrix elements between two different configurations from the experimental data. This has been possible in a few cases, but not enough systematic data exist for a convincing treatment.[3] A few comments on the behavior of 0^+ states in the Pb region are included in Sec. III. G.

In Sec. II, the experimental data used and the experimental two-body matrix elements deduced from them will be discussed. Section III will describe how a residual two-body interaction was determined and how well different residual interactions worked. A discussion of the results and conclusions will be given in Sec. IV.

II. EXPERIMENTAL DATA

The selection of the experimental data used in obtaining the two-body matrix elements is clearly important in determining the results of a survey such as the present one.

Since different components of the residual interaction contribute to the $T=0$ and $T=1$ matrix elements, it is convenient whenever possible to separate the $T=0$ from the $T=1$ matrix elements. The neutron–proton multiplets have contributions from both the $T=0$ and $T=1$ parts of the interaction. However, if one knows the $T=1$ matrix elements, which can be determined from the proton–proton, neutron–neutron, proton–proton–hole, or neutron–neutron–hole data, one can then calculate the $T=0$ matrix elements since

$$E_{J,\,\mathrm{np}}(j_1 j_2)=\frac{1}{2}\sum_{T=0,\,1} E_{J,T}(j_1 j_2). \qquad \text{(II.1)}$$

The matrix elements extracted from the data are given in the Appendix.

A. Selection of experimental data

The criteria used in selecting experimental data involve considerable judgment and ultimately have a subjective component. Whenever possible, results from one-nucleon transfer were taken, since in this reaction the configurational purity of nuclear states is measured through the spectroscopic factor. About 80% of the matrix elements used here have been determined through such reactions. The remainder were attained from (a) shell-model fits to a region of the periodic table, (b) the (^{3}He, t) reaction, which seems to have a certain amount of configurational selectivity, and (c) in one case the (^{3}He, p) reaction. A fair amount of information was excluded even where matrix elements are quoted in the literature but, in the authors' view, some substantial questions still exist. No cases were used where only two members of a $(j_1 j_2)_J$ multiplet are known. In the following are some of the more detailed considerations regarding the experimental data.

1. The $(1p_{3/2})^2$ and $(1p_{1/2}\,1p_{3/2})$ multiplets

These data were taken from the work of Cohen and Kurath (1965). Their shell-model calculations fit the data in the $1p$ shell remarkably well and have repeatedly demonstrated their accuracy by predicting not only energies but matrix elements for electromagnetic transitions and transfer reaction strengths. We included their matrix elements labeled "(8–16)2BME"; the alternate sets of matrix elements were not significantly different.

2. The $(1d_{5/2})^2$ matrix elements

Data on these are summarized in Table I for $A=18$, and in Table II for $A=26$ (which may be regarded as two holes in a complete $1d_{5/2}$ shell), and the comparison is made in Table III.

In $A=18$ most of the data comes from Polsky *et al.* (1969) and Wiza *et al.* (1966). The ^{17}O$(d,p)^{18}$O experiment was recently also reported (Li *et al.*, 1975) and the results of that analysis are given. Some obvious difficulties will be apparent. In particular the 0^+ matrix element has shifted because of an additional 0^+ state with an appreciable spectroscopic factor at 5.329 MeV in ^{18}O. Considerable uncertainty exists in the 1^+ strength: The one state with a clear $l=2$ transition is too weak to exhaust the sum rule limit, and two other known 1^+ states have not been analyzed in the one relevant experiment (Polsky *et al.*, 1969). There is likewise an uncertainty about the inclusion of a known 4^+ state at 7.114 MeV in ^{18}O, which Li *et al.* (1975) assign as belonging to the $(1d_{3/2}\,1d_{5/2})$ configuration. Clearly, polarization measurements would be of some help here. The uncertainty in the $l=2$ spectroscopic factors for the 0.937 MeV and 3.357-MeV 3^+ states likewise presents an uncertainty in the 3^+ matrix elements.

For $A=26$ somewhat analogous uncertainties exist. The $T=1$ matrix elements are apparently fairly well known from the ^{27}Al$(d,{}^3\mathrm{He})^{26}$Mg data of Wagner *et al.* (1969). The only uncertainty is in the 7.25-MeV state. For the $T=0$ transition, the ^{27}Al$(p,d)^{26}$Al data of Kroon *et al.* (1973) were used. In both cases the renormalized spectroscopic factors are split among the different J states very nearly in proportion to $(2J_f+1)$, indicating reasonable consistency.

The comparison of the two sets of matrix elements is made in Table III. The level of agreement is gratifying. The disagreement is worst for the 1^+ state, where the $A=18$ data are especially shaky. For the 0^+ state the level of agreement was spoiled by the recent work of Li *et al.* (1975). All one can say is that since these transitions are weak (because of the statistical factor) the un-

[3] Heusler and Brentano have extracted a set of particle-hole matrix elements, from isobaric analog data, for ^{208}Pb (Heusler and Brentano, 1973). The uncertainties in this procedure caused us not to include their matrix elements in our survey.

TABLE I. $(1d_{5/2})^2$ matrix elements in MeV from ^{18}O–^{18}F.

^{17}O(^{3}He, d)^{18}F. [a]		
E^*	J^π $(T=0)$	G [b]
0.0	1^+	0.37
0.937	3^+	<0.42
1.122	5^+	1.83 [c]
1.701	1^+	(0.02) [d]
3.357	3^+	(<0.06) [d]
3.724	1^+	(<0.01) [d]
4.119	3^+	0.88

Matrix elements from centroids			
J^π	E_J [e]	G [i]	Sum rule
0^+	−2.77	0.34	0.33
1^+	−5.01 (−4.19) [f]	0.37 (0.49) [f]	0.50
2^+	−1.06	1.53	1.67
3^+	−1.69 (−0.89) [g]	1.67 [g]	1.17
4^+	−0.36 (0.08) [h]	2.89 (3.13)	3.00
5^+	−3.89	1.83 [c]	1.83

[a] These data are from Polsky *et al.* (1969), the excitation energies from Ajzenberg-Selove (1972).

[b] For stripping $G \equiv [J_f]C^2S/[J_i]$, where J_i and J_f are the initial and final spins, C is the isospin Clebsch, and S is the spectroscopic factor (see Macfarlane and French, 1960 and Schiffer, 1969).

[c] Spectroscopic factors normalized to this value.

[d] Limits on $l=2$ spectroscopic factors were based on states whose spins are now known, on the basis of Fig. 1 of Polsky *et al.* (1969), which shows a 10° spectrum. These numbers were used only to set limits on the centroids.

[e] $T=1$ matrix elements from Li (1975) in ^{18}O with $E_0=3.904$ MeV. $T=0$ matrix elements are from ^{18}F with $E_0=5.008$ MeV.

[f] Value obtained by assuming that the higher 1^+ states were populated with the maximum spectroscopic factors allowed by the experimental limits.

[g] The first value is computed assuming that the G for the 0.937-MeV state is 0.29, the value needed to bring the sum up to the limit of 1.17. The value in parentheses corresponds to the 4.119-MeV state being *the* $(1d_{5/2})^2$ 3^+ state.

[h] Value obtained by assuming that the $l=2$ spectroscopic factor for the 7.114-MeV 4^+ state in ^{18}O is due to a $1d_{5/2}$ transfer.

[i] Values are for the (d,p) reaction for $T=1$ states and the $(^3\text{He}, d)$ reaction for $T=0$ ones. The (d,p) spectroscopic factors are renormalized so that the overall sum of them is equal to 5.0, the sum rule limit.

TABLE II. $(1d_{5/2})^2$ matrix elements in MeV from ^{26}Mg–^{26}Al.

^{27}Al(d, ^{3}He)^{26}Mg. [a]		
E^*	J^π	C^2S
0.0	0^+	0.27
1.809	2^+	0.92
2.938	2^+	0.19
3.588	0^+	0.01
4.320	4^+	1.95
4.835	2^+	0.36
5.474	4^+	0.32
6.127	2^+	0.14
7.25	(4^+) [b]	0.34
^{27}Al(p, d)^{26}Al [c]		
0.0	5^+	1.37
1.058	1^+	0.33
1.851	1^+	0.07
2.365	3^+	0.39
2.545	3^+	0.39
3.405	5^+	0.27

J^π	$\bar{E}_J$ [d]	G [e]	G (sum rule limit)
0^+	−3.65	0.31	0.33
1^+	−2.92	0.50	0.50
2^+	−0.71	1.79	1.67
3^+	−1.66	0.97	1.17
4^+	0.81 (1.17) [f]	2.52 (2.90) [f]	3.00
5^+	−3.56	2.04	1.83

[a] Spectroscopic factors from Wagner *et al.* (1969). The energies are from Endt and Van der Leun (1973).

[b] The spin assignment of the 7.25 state is not known. Perhaps it may be taken as 4^+ because it decays by gamma emission to 2^+ and 3^+ states and not to 0^+ states.

[c] Spectroscopic factors from Kroon *et al.* (1973) and energies from Endt and Van der Leun (1973).

[d] Energies computed from Eq. (I.1) with $E_0=3.315$ MeV for ^{26}Mg and 4.119 MeV for ^{26}Al. The ^{26}Mg matrix elements are corrected for Coulomb interaction; they are actually $E_J^{\text{Nucl}} \equiv E_J - E_J^{\text{Coul}}$. E_J^{Coul} was calculated with oscillator wave functions ($\nu=0.293$ fm^{-2}); the values were 0.461, 0.389, 0.362 MeV for $J=0$, 2, and 4, respectively.

[e] For pickup reactions $G \equiv C^2S$. The G values were normalized separately by requiring $\sum G$ for $T=1$ to be equal to 5, and 3.5 for the (p,d) reaction to $T=0$ states.

[f] The values in parentheses include the 7.25-MeV state.

certainties are large. There is also some, less serious, discrepancy in the 4^+ energies where some doubts exist in assignments. Table III gives some recommended values which are the weighted averages of the above.

3. The $(1p_{3/2}\,1d_{5/2})$ matrix elements

These data have been taken from the ^{17}O$(d, t)^{16}$O and ^{17}O$(d, ^3\text{He})^{16}$N data of Mairle (1972) (see also Mairle, 1974). In this, the $l=1$ transitions were analyzed, many of them to states of undetermined spin. Making very tentative assignments, with heavy reliance on shell-model calculations for prediction of admixtures, Mairle extracted the relevant particle–hole matrix elements. These should be regarded with considerably more caution than other data used in this study. On the other hand, it is the largest multiplet known for $A<34$ and is included for that reason. The details of Mairle's analysis are not reproduced here, and only the Pandya transform of his results is included in the Appendix. This multiplet was included with a very low weight in the fitting procedure.

4. The $(1d_{3/2})^2$ matrix elements

The data on these matrix elements were taken from Crozier (1972), where the data from ^{33}S$(d,p)^{34}$S are evaluated together with the ^{33}S$(^3\text{He}, d)^{34}$Cl data of Erskine *et al.* (1971). A comparison with other sources of $(1d_{3/2})^2$ matrix elements is given in those papers.

5. The $(1d_{3/2}\,1f_{7/2})$ matrix elements

These were taken from the same references as the $(1d_{3/2})^2$ matrix elements. It is interesting to note that

more recently the ^{38}Cl results have been shown to be consistent with those for $A = 38$ (Fink and Schiffer, 1974). Even in ^{40}Ca, where the ^{39}K(^{3}He, d)^{40}Ca data (Erskine, 1966; Seth *et al.*, 1967; Forster *et al.*, 1970) have been inconsistent with the $A = 34$ results (Crozier, 1972), recent work on ^{41}Ca(d, t)^{40}Ca (Cline *et al.*, 1974; Betts *et al.*, 1974) has shown additional states which tend to reduce the discrepancies. Although the ^{40}Ca odd-parity states are widely quoted as "the" $(1d_{3/2}^{-1}1f_{7/2})$ particle–hole states, the strengths of the transfer reactions indicate that the configurations are fragmented and that substantial fractions of the strength are still unidentified (e.g., the 3^-, $T = 0$ strength).

6. The $(1f_{7/2})^2$ matrix elements

There had been some controversy regarding the appropriate values to use for this case. Data have been available for some time for two nucleons outside ^{40}Ca in ^{42}Ca and ^{42}Sc and the lowest states of each spin had been taken as representing the $(1f_{7/2})^2$ multiplet (Schwartz, *et al.* 1967). But the values disagreed with those derived from the spectrum of ^{48}Sc, which may be regarded as a hole in a complete $(1f_{7/2})^8$ neutron shell coupled to a single $1f_{7/2}$ proton (Ohnuma *et al.*, 1970). Differences in the matrix elements are apparent as shown in Table IV, and arguments can be made in favor of ^{48}Sc on the basis of ^{48}Ca being a better closed core than ^{40}Ca, and on the basis of a comparison of the average interaction in $T = 0$ and $T = 1$ states with the values derived from the ground-state masses of ^{40}Ca, ^{48}Ca, and ^{56}Ni (Moinester *et al.*, 1969). The significance of the differences between ^{42}Sc and ^{48}Sc was also analyzed by West and Koltun (1969).

Unfortunately neither spectrum was accessible to single-nucleon transfer reactions. Recently, however, with the advent of a ^{41}Ca target, the $A = 42$ spectra have been reexamined (Hansen *et al.*, 1975; Vold *et al.*, 1974) and it was found that much of the ^{41}Ca(d, p)^{42}Ca and ^{41}Ca(^{3}He, d)^{42}Sc $l = 3$ strength was fragmented into higher states. Using the centroids of energies in $A = 42$, the agreement with the ^{48}Sc data is much improved, as may be seen in Table IV. Since the $A = 42$ information became available only recently, the matrix elements from $A = 48$ were used in the fitting procedure. The differences are not sufficient to alter the results in any case, and uncertainties in the $A = 42$ centroids are likely to be of the same order as the differences between $A = 42$ and $A = 48$ matrix elements.

TABLE III. Summary of $(1d_{5/2})^2$ matrix elements in MeV.

J^π	^{18}F–^{18}O [a]	^{26}Al–^{26}Mg [b]	Recommended value
0^+	−2.77	−3.65	−3.2
1^+	−5.01 (−4.19)	−2.92	−3.3
2^+	−1.06	−0.71	−0.9
3^+	−1.69 (−0.9)	−1.66	−1.6
4^+	−0.36 (0.08)	+0.81 (1.17)	+0.3
5^+	−3.89	−3.56	−3.7

[a] From Table I.
[b] From Table II.

7. The $(1f_{7/2}2p_{3/2})$ matrix elements

These data come from the low-lying levels of ^{50}Sc which were determined primarily from the ^{48}Ca(^{3}He, p)^{50}Sc reaction (Ohnuma *et al.*, 1969). Since this reaction does not distinguish configurations, the principal justification of this identification is the wide separation between the ground state and first-excited state, in both ^{49}Ca and ^{49}Sc. Since the proton is $1f_{7/2}$ and the neutron $2p_{3/2}$, this is an n–p multiplet. The expected purity of the configuration receives some support from shell-model calculations, where the calculated admixtures are ~5% (Kuo, 1968).

8. The $(1g_{9/2}2d_{5/2})$ multiplet

These matrix elements are taken as they appear in Fann *et al.* (1973). In that work the n–p matrix elements, from the particle–particle spectrum of ^{92}Nb (Ball and Cates, 1967; Zisman and Harvey, 1972; Bhatia *et al.*, 1971), and confirmed by the particle–hole spectrum of ^{96}Nb (Comfort *et al.*, 1970) as shown in Table V, is combined with the $T = 1$ (neutron–particle–neutron–hole) spectrum obtained from the ^{91}Zr(^{3}He, α)^{90}Zr reaction. The two n–p spectra are compared in particle–hole form; the agreement is almost perfect except for the 2^+ state, where one might expect some admixtures. This difference is distributed among all J states of the particle–particle spectrum by the Pandya transformation.

TABLE IV. $(1f_{7/2})^2$ matrix elements in MeV.

J^π	^{42}Sc [a]	^{42}Ca [b]	^{42}Sc [c]	$P\{^{48}\text{Sc}\}$ [d]	Closed shell masses [e]
			$T = 1$		
0^+	(−3.18)	−2.59	−2.89	−2.13	
2^+	(−1.59)	−0.94	−1.10	−0.81	
4^+	(−0.36)	−0.26	−0.26	+0.06	
6^+	(0.06)	+0.08	+0.07	+0.28	
$\bar{E}_{\text{even}}$ [f]	−0.49	−0.31	−0.35	−0.07	−0.25
			$T = 0$		
J^π	^{42}Sc [a]		^{42}Sc [c]	$P(^{48}\text{Sc})$ [d]	Closed shell masses [e]
1^+	(−2.56)		−1.68	−2.11	
3^+	(−1.68)		−0.82	−1.04	
5^+	(−1.66)		−0.80	−0.87	
7^+	(−2.56)		−2.56	−2.28	
$\bar{E}_{\text{odd}}$ [f]	−2.11		−1.61	−1.59	−1.49

[a] Values obtained by assuming that single states in ^{42}Sc represent the $(1f_{7/2})^2$ configuration, as was done by Schwartz *et al.* (1967). The more recent energies Endt and Van der Leun (1973) were used; $E_0 = 3.175$ MeV.
[b] Hansen *et al.* (1975). $E_0 = 3.110$ MeV.
[c] Vold *et al.* (1974).
[d] The Pandya transform of the $(\nu 1f_{7/2})^{-1}(\pi 1f_{7/2})$ spectrum from single states in ^{48}Sc. The energies and spins of Ohnuma *et al.* (1970) were used, $E_0 = -0.178$ MeV.
[e] Values computed from the ground-state masses of ^{40}Ca, ^{41}Ca, ^{41}Sc, ^{48}Ca, and ^{56}Ni as discussed in Moinester *et al.* (1969).
[f] $\bar{E}_{\text{even,odd}}$ are the $(2J+1)$-weighted average matrix elements for J = even, odd (or $T = 1$ and 0), respectively.

TABLE V. Comparison of the $(1g_{9/2}2d_{5/2})$ n–p multiplets in MeV derived from ^{92}Nb and ^{96}Nb.

	E_J			
J^π	$E^*(^{92}\text{Nb})$ [a]	$E^*(^{96}\text{Nb})$ [b]	$E_J^{p-h}(^{92}\text{Nb})$ [c]	$E_J^{p-h}(^{96}\text{Nb})$ [d]
2^+	0.136	0.630	0.987	0.866
3^+	0.286	0.180	0.418	0.416
4^+	0.480	0.142	0.388	0.378
5^+	0.357	0.043	0.268	0.279
6^+	0.500	0.0	0.232	0.236
7^+	0.0	0.233	0.451	0.469
E_0	0.691 [e]	−0.236 [f]		
$\bar{E}$ [g]	−0.401	+0.400		

[a] Energies from Kocher and Horen (1972); see also Sheline *et al.* (1964).
[b] Energies from Medsker (1972).
[c] Pandya transform of the first column with E_0 subtracted.
[d] The excitation energies of the second column, with E_0 subtracted.
[e] Computed from the ground-state binding energies of ^{91}Zr, ^{91}Nb, and ^{97}Nb.
[f] Computed from the ground-state binding energies of ^{95}Zr, ^{97}Nb, and ^{96}Nb.
[g] The $(2J+1)$-weighted centroid of the excitation energies with E_0 subtracted.

9. The $(1g_{9/2})^2$ multiplet

These data are taken from ^{90}Nb, where the relevant states were observed in a very clear pattern in the ^{90}Zr(^{3}He, t)^{90}Nb reaction (Bearse *et al.*, 1969). This reaction does seem to have a special selectivity for particle–hole excitations, as was already discussed in the analogous case of ^{48}Sc. Some worries exist as the ground state of ^{90}Zr is not a good closed proton shell. Admixtures of $(2p_{1/2})^{-2}(1g_{9/2})^2$ (~40%) and $(2p_{3/2})^{-2}(1g_{9/2})^2$ (~20%) seem to be required (Courtney and Fortune, 1972). This may imply some admixtures of, for instance, $(\pi 1g_{9/2})^3(\nu 1g_{9/2})^{-1}$ in ^{90}Nb and $(\pi 1g_{9/2})^3$ in the single-particle energy in ^{91}Nb. That such admixtures do not seem to alter the results significantly is supported from two sources.

The first is an experimental study of ^{88}Y (Comfort and Schiffer, 1971), a nucleus which should be the same as ^{90}Nb but without the troublesome proton pair; indeed $Z = 38$ seems a better closed shell than $Z = 40$. This nucleus has the additional experimental advantage that it is accessible to proton transfer reactions from the stable $(\nu 1g_{9/2})^{-1}$ ground state of ^{87}Sr. Both the (^{3}He, d) and (α, t) reactions were studied from this target together with the ^{88}Sr(^{3}He, t)^{88}Y reaction. Unfortunately, the accidental proximity of several levels and the fragmentation of others makes this a less simple case to interpret than ^{90}Nb, but the results are certainly consistent, as may be seen from Fig. 1. The second confirmation comes from shell-model calculations in this vicinity. The results of Serduke *et al.* (1975) indicate that the matrix elements obtained in a least-squares fit are indeed close to the ones we obtained directly from ^{90}Nb.

10. The $(\pi 1h_{9/2}\nu(3p_{3/2}, 2f_{5/2}, 2f_{7/2}, 1i_{13/2})^{-1})$ n–p multiplets

These are all from ^{208}Bi, obtained from neutron pick-up reactions on ^{209}Bi. The first two multiplets were first identified by Erskine (1964). All four were seen by Alford *et al.* (1968 and 1971) and Crawley *et al.* (1973). The spin assignments for many of the lower states have been confirmed by gamma-ray measurements. The level of agreement among the measurements is good; Crawley *et al.* (1973) assigns some of the members of the $(1h_{9/2}1i_{13/2})$ multiplet differently from the earlier work. We adopt the later measurements. The transfer reactions indicate all these multiplets to be remarkably pure (> 95% in terms of the corresponding states in ^{207}Pb) and free of admixtures. The energies corresponding to these multiplets are listed in Table VI.

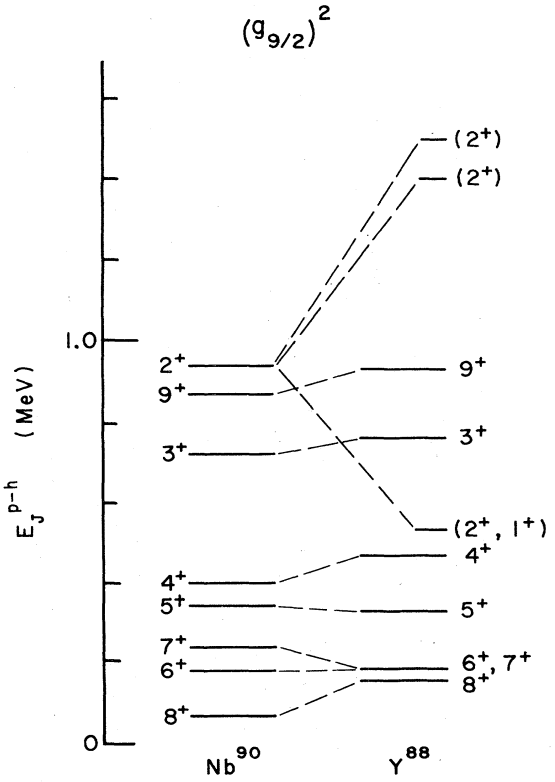

FIG. 1. Comparison of data on the $(1g_{9/2})^2$ matrix elements from ^{90}Nb with partial data from ^{88}Y (Comfort and Schiffer, 1971).

11. The $(\pi 1h_{9/2}\nu 2g_{9/2})$ n–p multiplet

This multiplet has been known for some time (Erskine *et al.*, 1962) from the ^{209}Bi(d, p)^{210}Bi reaction. The multiplet appears to be pure and subsequent measurements have left the original assignments unchanged.

12. The $(1h_{9/2}\,1i_{13/2})$ and $(1h_{9/2}2f_{7/2})T=1$ multiplets

These data come from the ^{209}Bi(^{3}He, d)^{210}Po and ^{209}Bi(α, t)^{210}Po reactions, in a regrettably unpublished experiment (Lanford *et al.*, 1971). In independent gamma-ray experiments, Fant (1971), apparently unaware of Lanford's work, confirmed many of his assignments. The ^{209}Bi(α, t)^{210}Po reaction has been studied by Tickle and Bardwick (1971) with lower resolution; no unique assignments could be made though the results are consistent with Lanford's.

Since the two $T = 1$ multiplets in ^{210}Po involve two protons, the Coulomb interaction between these has to be subtracted. This is done in Table VII. These $T = 1$ matrix elements then may be combined with the n–p matrix elements of ^{208}Bi to yield the $T = 0$ matrix elements as well.

13. The $(1h_{9/2})^2$ and $(2g_{9/2})^2$ $T=1$ multiplets

These are known quite well from the low-lying spectra of ^{210}Po (Lanford *et al.*, 1971) and ^{210}Pb (Bjerregaard *et al.*, 1968). The difficulty is that the 0^+ ground states contain large admixtures of other configurations because of pairing correlations and so their energies are significantly lower than those of pure $(2g_{9/2})^2_0$ or $(1h_{9/2})^2_0$ states. In fact, the ^{210}Pb ground state is used as a prototype of the pairing-vibration model (Bohr, 1968; Nathan, 1972).

In principle, transfer reactions could identify the other relevant components of this configuration scattered among the 0^+ states at higher excitation, but this does not work in practice since the one-nucleon transfer statistical factor insures that only ~2% of the single-particle strength is contained in the 0^+ states in the first place, and the relevant higher 0^+ states have not so far been identified. The 2^+ state may likewise suffer from collective admixtures, but the higher spin members of these multiplets are likely to be increasingly pure. The results are given in Table VIII. For ^{210}Pb, no single-neutron transfer reaction is practical; ^{210}Po was studied by proton stripping on ^{209}Bi. These matrix elements were included in the fitting procedure with substantially reduced weight.

TABLE VI. Multiplets in MeV derived from ^{208}Bi. [a]

Configuration	E_0 [b]	J^π	E^* [c]	E_J^{n-p} [d]	E_J^{n-p} [e]
$1h_{9/2}3p_{1/2}^{-1}$	−0.085	4^+	0.063	0.148	−0.079
		5^+	0.000	0.085	−0.142
$1h_{9/2}3p_{3/2}^{-1}$	0.812	3^+	1.070	0.258	−0.304
		4^+	0.960	0.148	−0.119
		5^+	0.887	0.075	−0.100
		6^+	1.096	0.284	−0.222
$1h_{9/2}2f_{5/2}^{-1}$	0.484	2^+	0.926	0.442	−0.264
		3^+	0.634	0.150	−0.063
		4^+	0.603	0.119	−0.060
		5^+	0.629	0.145	−0.140
		6^+	0.510	0.026	−0.043
		7^+	0.650	0.166	−0.291
$1h_{9/2}2f_{7/2}^{-1}$	2.255	1^+	2.892	0.637	−0.670
		2^+	2.508	0.253	−0.429
		3^+	2.464	0.209	−0.208
		4^+	2.391	0.136	−0.210
		5^+	2.391	0.136	−0.116
		6^+	2.415	0.160	−0.184
		7^+	2.346	0.091	−0.058
		8^+	2.668	0.413	−0.340
$1h_{9/2}1i_{13/2}^{-1}$	1.548	2^-	2.901	1.353	−1.563
		3^-	1.925	0.377	0.727
		4^-	1.844	0.296	0.367
		5^-	1.708	0.160	−0.312
		6^-	1.721	0.173	−0.147
		7^-	1.721	0.173	−0.229
		8^-	1.664	0.116	−0.080
		9^-	1.792	0.244	−0.279
		10^-	1.571	0.023	−0.052
		11^-	2.434	0.886	−0.678
$2f_{7/2}3p_{1/2}^{-1}$	0.811	3^+	0.939	0.128	−0.239
		4^+	1.038	0.227	−0.140
$1i_{13/2}3p_{1/2}^{-1}$	1.523	6^-	1.630	0.107	−0.153
		7^-	1.673	0.150	−0.110
$2f_{5/2}3p_{1/2}^{-1}$	2.737	2^+	2.945	0.208	−0.144
		3^+	2.890	0.153	−0.199

[a] From Alford *et al.* (1971) and Crawley *et al.* (1973).
[b] From the binding energies of the relevant states in ^{207}Pb and ^{209}Bi.
[c] Energies are for the low-lying states Lewis (1971), otherwise from Alford or Crawley. In the few cases where the latter two disagree in assignments, the latter has been followed.
[d] Particle–hole energies.
[e] Pandya transform of the previous column.

14. Multiplets based on $(\nu 3p_{1/2}^{-1}\pi j)$

Doublets with such configurations have been identified in ^{208}Bi by Alford *et al.* (1971) through the ^{207}Pb(^{3}He, d) and $(\alpha, t)^{208}$Bi reactions. These doublets were included with a very low weight of 0.1; thus they play effectively no role in the fitting procedure. They are included in Table VI.

15. Other multiplets in ^{210}Bi

The $(1h_{9/2}1i_{13/2})$ multiplet was identified via the (n,γ) reaction (Motz *et al.*, 1971) though the (n,γ) reaction has no particular selectivity for such a configuration. The calculations of Kim and Rasmussen (1963) were used as a guide in this identification. A study of the ^{209}Bi$(d,p)^{210}$Bi and ^{209}Bi$(\alpha, ^3\text{He})^{210}$Bi reactions was carried out by Cline *et al.* (1972), who identified a number of $l = 6$ $(1h_{9/2}1i_{13/2})$ and $l = 7$ $(1h_{9/2}1j_{15/2})$ transitions as well as the $l = 4$ $(1h_{9/2}2g_{7/2})$ and $l = 2$ $(1h_{9/2}3d_{3/2})$ and $(1h_{9/2}3d_{5/2})$ levels, with some admixing between the $l = 4$ and $l = 2$ transitions. To assign spins, Cline *et al.* (1972) had to assume a number of unresolved doublets, and they also seem to have relied to some extent on the shell-model calculations of Kim and Rasmussen (1963) and Kuo and Herling (1971). These assignments seem more tentative than most we have accepted in the present study. There is little correspondence between the assignments of Motz *et al.* (1971) and Cline *et al.* (1972); these multiplets are not included here.

B. General features in the experimental matrix elements

Several comparisons of the experimental matrix elements seem worthwhile before embarking on detailed analyses. To gain a qualitative impression of spectra we adopt plots of matrix elements as a function of θ_{12}, the classical angle of orientation between the two angular momentum vectors j_1 and j_2 coupled to J which gives a measure of the overlap of their orbital wavefunctions. θ_{12} is defined by

$$\cos\theta_{12} = \frac{J(J+1) - j_1(j_1+1) - j_2(j_2+1)}{2\sqrt{j_1 j_2(j_1+1)(j_2+1)}} . \qquad \text{(II.2)}$$

In Figs. 2 and 3 we see the data plotted for which $j_1 = j_2$. The matrix elements were divided by the average

TABLE VII. The $(1h_{9/2}2f_{7/2})$ and $(1h_{9/2}1i_{13/2})$ multiplets in MeV.

J^π	E^* [a]	G [b]	E_J^{Coul} [c]	$E_J^{T=1}$ [d]	$E_J^{\text{n-p}}$ [e]	$E_J^{T=0}$ [f]
	$1h_{9/2}2f_{7/2}$					
1^+	2.284 (~2.400)	0.41 (0.3)	0.243	−0.032	−0.670	−1.308
2^+	~2.400 [g] (2.284)	(0.5)	0.230	0.097	−0.429	−0.955
3^+	2.409 [h]	0.58 (0.7)	0.216	0.120	−0.208	−0.536
4^+ [i]	2.383 [h]	1.04 (0.9)	0.210	0.100	−0.210	−0.520
5^+ [i]	2.403 [h]	1.46 (1.1)	0.203	0.127	−0.116	−0.359
6^+ [i]	2.325	1.33 (1.3)	0.204	0.048	−0.184	−0.416
7^+ [i]	2.438 [h]	1.46 (1.5)	0.203	0.162	−0.058	−0.278
8^+ [i]	2.188	1.72 (1.7)	0.230	−0.115	−0.340	−0.565
	$1h_{9/2}1i_{13/2}$					
2^-	2.849 [j] (3.010)	(0.5)	0.248	−0.182 (−0.020)	−1.563	−2.944
3^-	3.010 [j] (2.849)	(0.7)	0.230	−0.002 (−0.163)	−0.727	−1.452
4^-	3.072	0.7 (0.9)	0.215	0.075	−0.367	−0.809
5^- [i]	3.027 [j] (2.97)	(k) (1.1)	0.209	0.036 (−0.024)	−0.312	−0.660
6^- [i]	3.123	1.2 [k] (1.3)	0.200	0.140	−0.147	−0.433
7^- [i]	3.013	3.1 [l] (1.5)	0.198	0.036	−0.229	−0.494
8^- [i]	3.138	1.7 [k] (1.7)	0.194	0.162	−0.080	−0.322
9^- [i]	3.000	1.5 [l] (1.9)	0.199	0.019	−0.279	−0.577
10^- [i]	3.182	2.3 (2.1)	0.199	0.201	−0.052	−0.305
11^- [i]	2.849	3.0 (2.3)	0.233	−0.166	−0.678	−1.190

[a] From Lanford *et al.* (1971).

[b] $G \equiv [(2J_f+1)/(2J_i+1)]C^2S$. The values represent those of Lanford *et al.* (1971), normalized such that $\sum_J G_J$ is equal to the sum rule limit. For the $1h_{9/2}2f_{7/2}$ multiplet, both (^{3}He, d) and (α,t) results are available, and the average was used. The expected value of G for each value of J is given in parentheses.

[c] Coulomb matrix elements were calculated with oscillator wave functions using $\nu = 0.1578$ fm^{-2}.

[d] $E_J^{T=1} \equiv E_J^* - E_0 - E_J^{\text{Coul}}$, where $E_0 = 2.073$ and 2.782 MeV, respectively, for the $1h_{9/2}2f_{7/2}$ and $1h_{9/2}1i_{13/2}$ multiplets as calculated from the binding energies of the appropriate state in ^{209}Bi.

[e] Pandya transform of the particle-hole multiplets of Table VIII.

[f] Computed from $E_J^{\text{n-p}} = \frac{1}{2}(E_J^{T=0} + E_J^{T=1})$.

[g] The excess strength in G under the known 4^+ and 5^+ states at 2.383 and 2.409 MeV (0.5) is the correct amount for the missing 2^+ state. The possibility that the 1^+ and 2^+ assignments are interchanged still cannot be ruled out, as is indicated.

[h] These states are only partially resolved in the transfer reactions.

[i] States and spins identified in gamma-ray measurements (Fant, 1971).

[j] The 2^- and 3^- assignments are based on excess strength in G observed under the 11^- state (0.7) and the $9^-, 7^-, 5^-$ group (<1.2), at 3.000, 3.016, 3.027 MeV. The 2^- and 3^- states could be inverted. Two 5^- states were identified by Fant (1971) at 2.910 and 3.026 MeV. On the basis of population of these states in electron capture he suggests that the former is primarily the 5^- excited state [3.198 MeV of ^{208}Pb coupled to the ground-state proton configuration of ^{210}Po $(1h_{9/2})_0^2$]. But Lanford sees a state at this energy with $G \approx 0.5$, suggesting a strong mixing between these 5^- levels. The centroid of the two energies adopted here gives a 58-keV lower value for the 5^- excitation energy (2.969 MeV) than is obtained with the Lanford–Fant assignment for the 3.026-MeV state.

[k] The 5^-, 6^-, and 8^- states are known from gamma-ray work. The split of spectroscopic strength between 6^- and 8^- states is based on partially resolved lines in the (α,t) spectrum.

[l] The 7^- and 9^- states are known from gamma-ray work. The split of spectroscopic strength between 7^- and 9^- states is based on partially resolved lines in the (α,t) spectrum.

interaction energy $\bar{E} \equiv \sum_J [J]E_J / \sum_J [J]$ as this provides a natural scaling to account for the different size of the matrix elements. The behavior we see is characteristic of a short-range attractive force where for $T = 0$ the matrix elements become large when θ_{12} approaches 0° and 180° (J has its maximum and minimum value). In these limits the orbits are nearly coplanar, and thus the overlap of the orbits is maximal. For the $T = 1$ matrix elements in Fig. 3 this is true toward $\theta \approx 180°$ ($J = 0^+$) but not for the high spin states toward low θ. The reason for this is that for high J, $T = 1$ implies approximate spatial antisymmetry; even though the orbits become coplanar, the particles may be thought of as rotating in the same sense but out of phase with each other, the separation between them is always large, and thus the interaction matrix element approaches zero with a short-range force. For the 0^+ state the rotation is of course in opposite directions; thus the overlap is large. The $j_1 = j_2$ data are replotted in Fig. 4 multiplet by multiplet, for later comparison with calculations.

The similarity in the behavior of the various multiplets is indeed striking, considering that they span nuclei from the $1p$-shell where $A \approx 12$ to $A = 90$. The major apparent discrepancy in Fig. 3 is in the relative energies of the various 0^+ states. Closer inspection reveals that these are, in fact, ordered by j. The $(1g_{9/2})_{0^+}^2$ matrix element in Fig. 3 is the largest and the $(1d_{3/2})_{0^+}^2$ and

TABLE VIII. The $(1h_{9/2})^2$ and $(2g_{9/2})^2$ $T = 1$ matrix elements in MeV from $A = 210$.

J^π	$(2g_{9/2})^2$ E^* [a]	$(2g_{9/2})^2$ E_J [b]	$(1h_{9/2})^2$ E^* [c]	$(1h_{9/2})^2$ E_{Coul} [d]	$(1h_{9/2})^2$ E_J [e]
0^+	0.0	−1.244	0.0	0.268	−1.442
2^+	0.795	−0.449	1.180	0.230	−0.224
4^+	1.091	−0.153	1.426	0.207	0.045
6^+	1.194	−0.050	1.472	0.196	0.102
8^+	1.273	0.029	1.552	0.195	0.183

[a] Energies and tentative spin and configuration assignments from Lewis (1971).

[b] With respect to $E_0 = 1.244$ MeV.

[c] Energies from Lewis (1971). Configuration and spin assignments from Tickle and Bardwick (1971) and Lanford *et al.* (1971).

[d] Two-body Coulomb energies calculated with oscillator wave functions using $\nu = 0.157\,86$ fm^{-2}.

[e] $E_J = E^* - E_{\text{Coul}} - E_0$ with $E_0 = 1.174$ MeV.

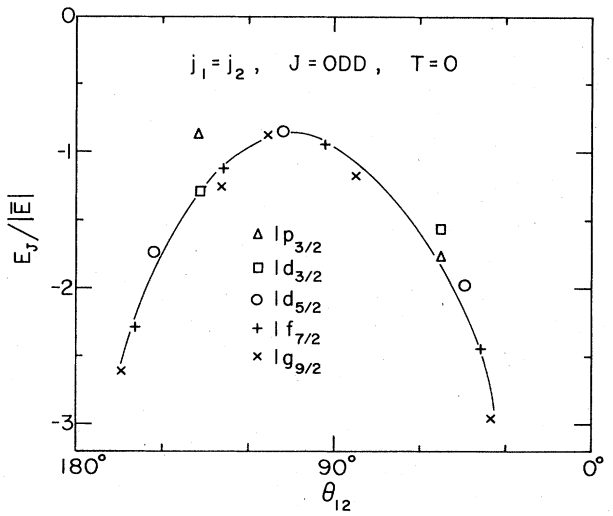

FIG. 2. Comparison of data from various multiplets with $j_1 = j_2$ and $T = 0$. The values of the matrix elements are divided by $\bar{E} \equiv \sum_J [J] E_J / \sum_J [J]$ to display the similarities in the J dependence (or θ dependence) of the various multiplets.

$(1p_{3/2})^2_{0^+}$ the smallest. This is precisely the behavior to be expected from a short-range force; the higher the j value, the better defined the orbital planes and the better the overlap of the wave functions when coupled to 0^+.

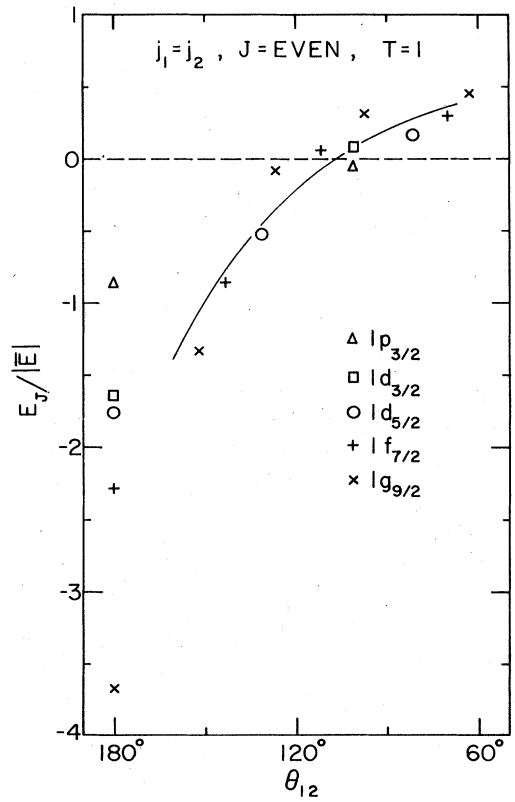

FIG. 3. Comparison of data from various multiplets with $j_1 = j_2$ and $T = 1$. The values of the matrix elements are divided by $\bar{E} \equiv \sum_J [J] E_J / \sum_J [J]$ to display the similarities in the J dependence (or θ dependence) of the various multiplets.

Next we consider cases where $j_1 \neq j_2$. The six such multiplets, in which matrix elements for all J values in both isospins are available, are shown in Figs. 5 and 6. Though there are some similarities, the pattern seems to be changing with increasing atomic weight. The inverted U shape of the $T = 0$ matrix elements persists in general, but the $T = 1$ matrix elements vary considerably, except in that their centroids are always repulsive (positive) and the matrix elements for the minimum and maximum J values are generally attractive (negative). Qualitatively this pattern indicates a $T = 1$ effective interaction that on the average is slightly repulsive but has a short-range attractive component which wins out over the repulsive component when the overlap between the two wave functions is good. The $T = 1$, $j_1 = j_2$ orbits also show this trend; the high-J matrix elements are always repulsive but an attractive interaction wins out for the 2^+ states and completely dominates the 0^+ ones. In general, the average interaction in $T = 1$ is weaker than in $T = 0$; the difference becomes more pronounced in the heavy nuclei. The data for multiplets where only the isospin-averaged n–p matrix elements are known, are plotted in Fig. 7.

1. The trends in the average (monopole) interaction

To study the average size of matrix elements one may compute $\bar{E}$ for the various multiplets. The trend is for the matrix elements to become smaller with increasing A, which, of course, is to be expected because the size of the orbits becomes larger while the interaction has constant range. The orbit size depends on three factors, the radius of the potential well, the binding of the orbit, and the quantum numbers of the orbit. In an oscillator potential the mean-square radius of an orbit is given by $\langle r^2 \rangle = \nu^{-1}[N + 3/2]$, where $N \equiv 2(n-1) + l$. More realistic finite wells show approximately the same dependence. The orbits we are concerned with are valence orbits so their binding energy is about constant and the radius of the relevant nuclei changes relatively slowly. In Fig. 8, the average $T = 0$ energies are plotted as a function of the sum $N_1 + N_2$ for the two orbits; this sum approximately increases with increasing A. The points fall on a remarkably smooth curve with the points for $j_1 = j_2$ and $j_1 \neq j_2$ multiplets exhibiting the same trend.

A similar plot for the $T = 1$ data in Fig. 9 shows a different smooth behavior, but with a definite difference between the identical-orbit and the nonidentical-orbit multiplets. The $T = 1$ trend is consistent with two competing ranges: for light nuclei the short-range attraction wins out; this is overcome by the longer-range repulsion in medium-weight nuclei, but the magnitude of the repulsion decreases slowly as the orbits become even larger.

2. Multipole decompositions

To study the more complex aspects of the shape of the spectra one can perform a multipole decomposition following Racah (1942). The notation of Moinester *et al.* (1969) will be used here.

The multipole coefficients

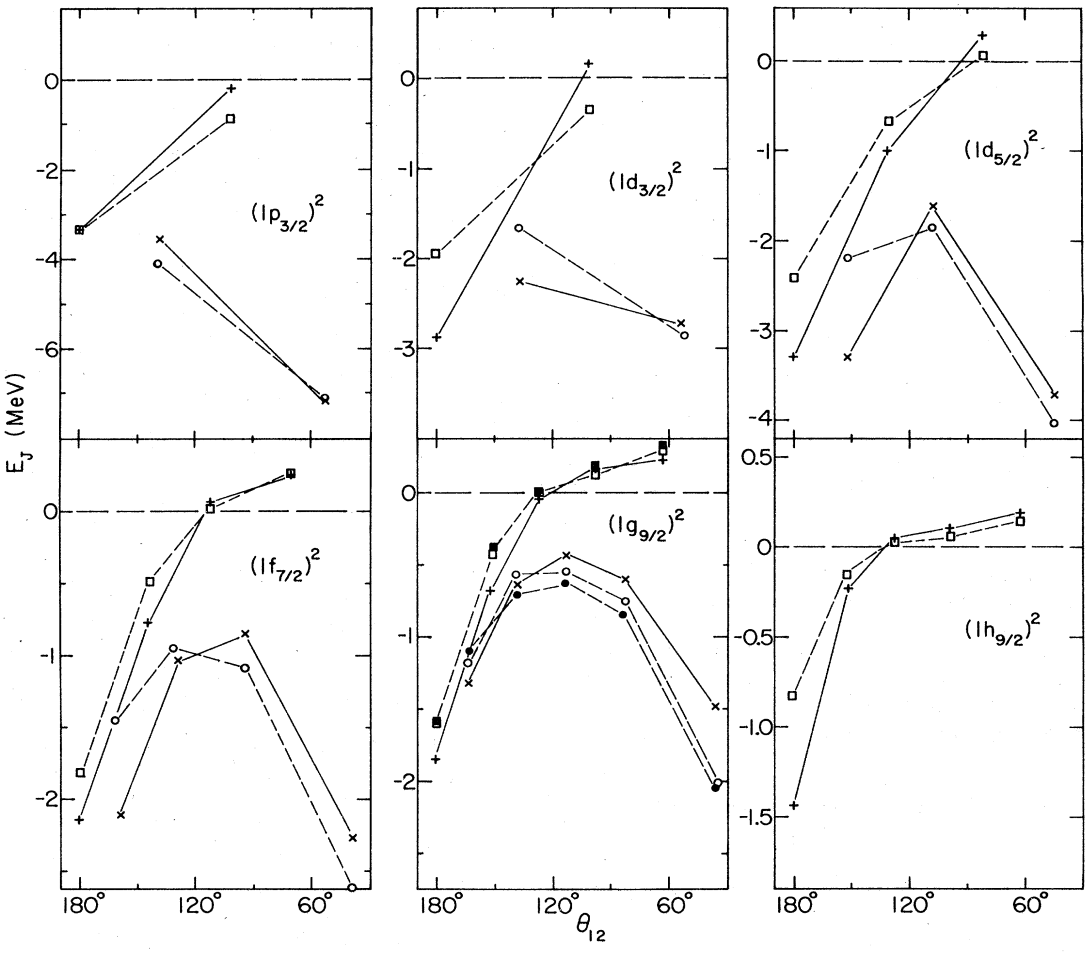

FIG. 4. Plots of the various $j_1=j_2$ multiplets. The data (crosses) are compared to calculations (circles for $T=0$ and squares for $T=1$) with the 12-parameter interaction of Table XVII ($r_2=2.0$ fm). The solid points for the $(1g_{9/2})^2$ multiplet represent calculations with the purely central five-parameter interaction of Table XIII.

$$\gamma_{KT} \equiv (-1)^{j_1+j_2}\left(\frac{[K]}{[j_1 j_2]}\right)^{1/2} \times \sum_J (-1)^J [J] W(j_1 j_2 j_1 j_2; JK) E_{J,T}(j_1 j_2) \qquad \text{(II.3)}$$

may first be defined separately in the two isospin states. Alternatively one can define multipole coefficients with a Racah coefficient that takes isospin explicitly into account. The resulting coefficients, α_{KT}, are simply related to the γ_{KT} by

$$\alpha_{K0}=\tfrac{1}{2}(\gamma_{K0}+3\gamma_{K1}) \text{ and } \alpha_{K1}=\tfrac{1}{2}(\gamma_{K1}-\gamma_{K0}).$$

Thus α_{K0} and α_{K1} may be called the isoscalar and isovector multipole coefficients. For the n–p multiplets

$$\gamma_{K\mathrm{np}}=\tfrac{1}{2}(\gamma_{K0}+\gamma_{K1}),$$

and for the particle–hole multiplets

$$\gamma_{K\mathrm{np}}^{(\mathrm{p\text{-}h})}=\gamma_{K,\mathrm{np}}^{(\mathrm{p\text{-}p})}(-1)^{K+1},$$
$$\gamma_{K0}^{(\mathrm{p\text{-}h})}=\tfrac{1}{2}(-\gamma_{K0}^{(\mathrm{p\text{-}p})}+3\gamma_{K1}^{(\mathrm{p\text{-}p})})(-1)^{K+1},$$
$$\gamma_{K1}^{(\mathrm{p\text{-}h})}=\tfrac{1}{2}(\gamma_{K0}^{(\mathrm{p\text{-}p})}+\gamma_{K1}^{(\mathrm{p\text{-}p})})(-1)^{K+1}.$$

Several features of the multipole coefficients should be noted. The rate of falloff of the even coefficients with increasing K is a measure of the range of the interaction. The longer the range the larger the monopole coefficient, compared to the higher multipoles, while for a delta function interaction all coefficients contribute with $\gamma_K \sim [K]^{-1/2}$. The odd coefficients (without isospin) are a direct measure of the spin dependence of the interaction.

The multipole coefficients for the multiplets with more than two matrix elements in each isospin are given in Tables IX and X. In general, their detailed behavior has not been especially helpful, except in providing qualitative insights. One such insight is illustrated in Fig. 10 where the isospin dependence of the interaction is plotted in terms of the even isovector coefficients for the four multiplets in which $j_1 \neq j_2$ and both isospin states are known. One should note that for the lighter nuclei the isovector monopole coefficient completely dominates, while in the Pb region the higher even-K isovector coefficients also take on finite values, indicating a finite range to the isospin dependent interaction.

Unfortunately the $j_1=j_2$ coefficients cannot be subjected to the same multipole analysis as the ones where

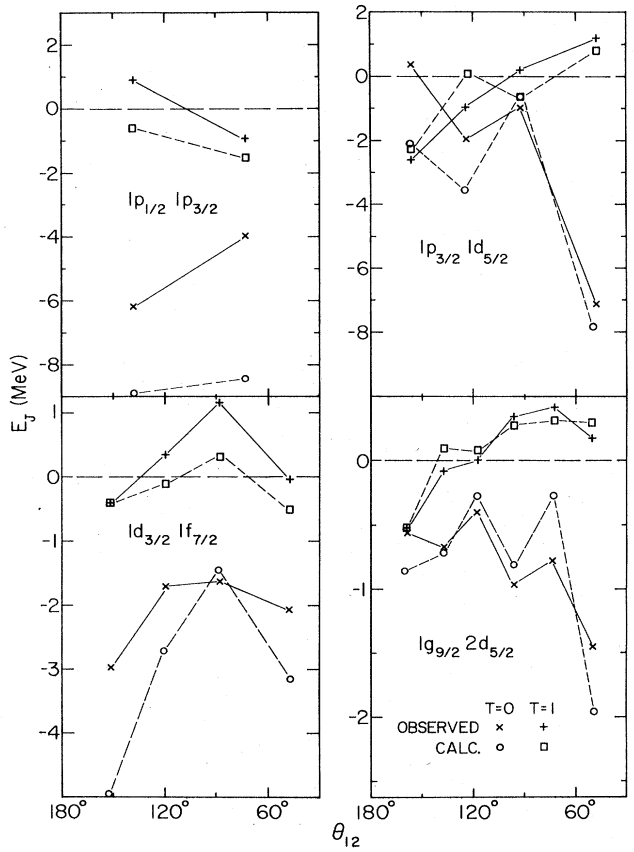

FIG. 5. Plots of some of the multiplets for $j_1 \neq j_2$ where information in separate isospin states is available. The $(1p_{3/2}1d_{5/2})$ data from $A = 16$ are rather more tentative than the rest. The upper left data are from the shell-model fits in the $1p$ shell. The lower left and lower right are from $A = 34$ and $A = 90, 92, 96$, respectively. The symbols have the same meaning as in Fig. 4.

$j_1 \neq j_2$, since only half the matrix elements exist because of the Pauli principle. If one had a complete set, say the $(1f_{7/2})^2$, $(1f_{5/2})^2$, and $(1f_{5/2}1f_{7/2})$ matrix elements, one could extract a set of direct and exchange Slater integrals, closely related to the multipole coefficients, but such complete data sets do not exist. Attempts to solve for a limited set of multipole coefficients, constraining either the odd-K coefficients or the coefficients with $K > j - \frac{1}{2}$ to be zero, have not yielded sensible results for $T = 1$. The $T = 0$ results are included in Table IX. As was discussed above in Sec. II.B, the qualitative behavior of all the $j_1 = j_2$ matrix elements is the same as that of the others.

The behavior of the multipole coefficients for the n–p multiplets is consistent with a short-range (delta function) interaction, as was noted by Moinester *et al.* (1969). Only when the matrix elements in different isospin states become known are additional features revealed which require a more complicated interaction.

III. FITTING THE EXPERIMENTAL MATRIX ELEMENTS TO AN EFFECTIVE INTERACTION

In order to connect all the data, a least-squares fitting procedure was used to find a single interaction which best fitted the observed matrix elements. The calculated matrix elements for each type of interaction (singlet, triplet, tensor, LS, even and odd) were used in a fitting program in which the strengths of the various interactions that would best fit the experimental data were obtained.

All calculated matrix elements used single-particle wave functions where the radial part had a harmonic-oscillator shape as discussed in Sec. III.B. The size of these orbits was fixed by requiring that the mean-square radius of all the occupied proton orbits be equal to the measured mean-square radius of the charge distribution in the relevant nuclide. The oscillator

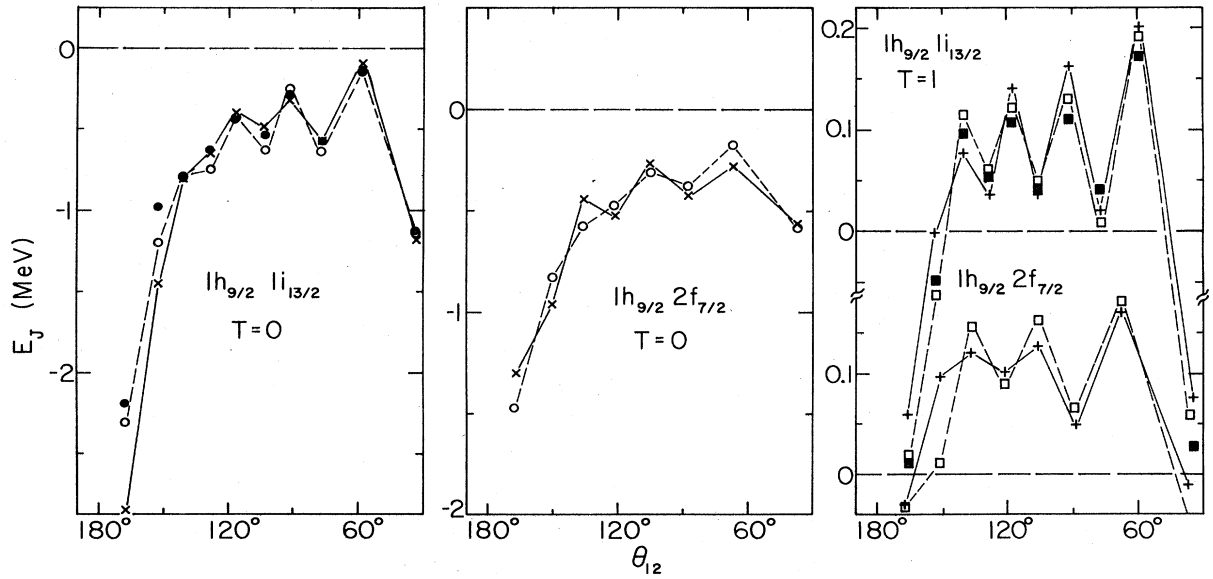

FIG. 6. Multiplets from the vicinity of ^{208}Pb where $j_1 \neq j_2$ and the matrix elements in both isospin states are known. The symbols have the same meaning as in Fig. 4.

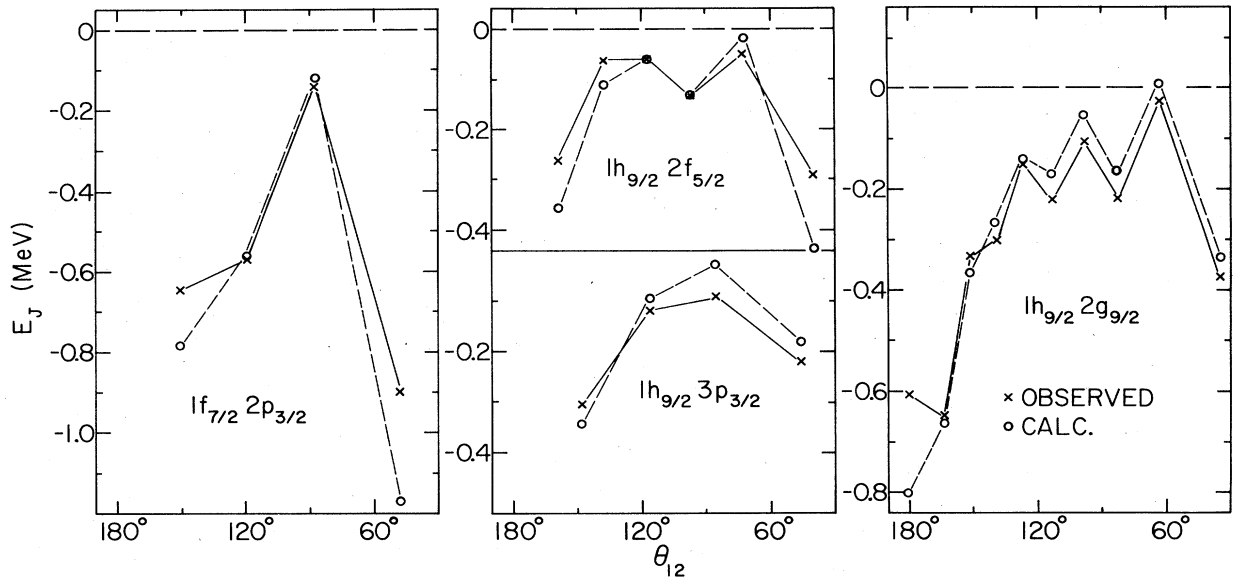

FIG. 7. Multiplets with $j_1 \neq j_2$ which are of the mixed isospin (n–p) type. The left-hand multiplet is from ^{50}Sc, the rest from the vicinity of ^{208}Pb.

strengths used are given in Table XII.

The central terms in the interaction were assumed to be sums of no more than two Yukawa shapes

$$U(r) = V_1 e^{-x_1}/x_1 + V_2 e^{-x_2}/x_2, \tag{III.1}$$

where

$$x_n \equiv r/r_n$$

with r_1 fixed at the one-pion-exchange value of 1.415 fm. For the noncentral interactions only one Yukawa shape was used with $r_1 = 1.415$ fm, giving a total of twelve parameters. The quantity

$$\chi^2 = \sum_i W_i \left(\sum_j V_j \epsilon_{ij} - E_i \right)^2 \tag{III.2}$$

was obtained where the various interactions j, with unit strength, have matrix elements ϵ_{ij} for a given state i, the experimental energies are E_i, and the weights attached to them are W_i. The strengths of the interactions V_j corresponding to the minimum value of χ^2 were obtained by solving the 12×12 determinant from the condition $\partial\chi^2/\partial V_j = 0$.

A. Properties of calculated interactions

The nucleon–nucleon interaction may be separated into two classes: central and noncentral. In Sec. III.B we will describe the methods used in this work in computing matrix elements to fit the experimental data; in the present section we discuss some of the properties of the computed matrix elements.

The central interaction can conveniently be decomposed into four parts and there are three equivalent representations which are normally used in practice. One such representation is the Wigner–Majorana–Bartlett–Heisenberg representation:

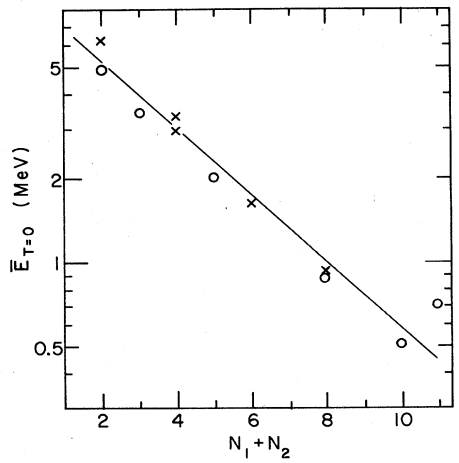

FIG. 8. The average interaction energy for $T = 0$ plotted against $N_1 + N_2$, where $N \equiv 2n + l - 2$. The crosses represent $j_1 = j_2$, the circles $j_1 \neq j_2$ multiplets. The line is drawn to show the average trend.

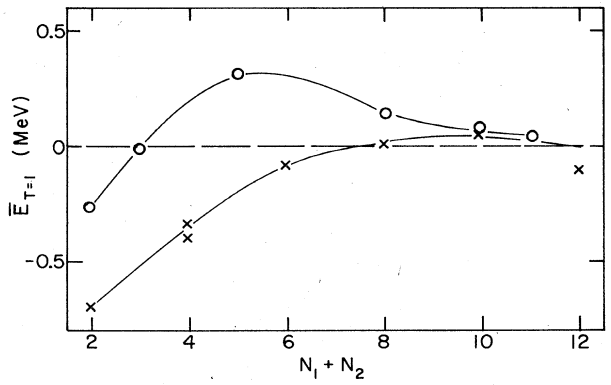

FIG. 9. The average interaction energy for $T = 1$ plotted against $N_1 + N_2$. The symbols have the same meaning as in Fig. 8.

TABLE IX. Multipole coefficients for $T=0$. [a]

Multiplet	$\gamma_{0,0}$ (MeV)	$\gamma_{1,0}/\gamma_{0,0}$	$\gamma_{2,0}/\gamma_{0,0}$	$\gamma_{3,0}/\gamma_{0,0}$	$\gamma_{4,0}/\gamma_{0,0}$
$1p_{3/2}1d_{5/2}$	−3.33	0.80	0.31	0.28	
$(1d_{5/2})^2$	−2.58	0.14	0.33		
$1d_{3/2}1f_{7/2}$	−2.00	−0.08	0.21	−0.07	
$(1f_{7/2})^2$	−1.46	−0.20	0.34	−0.10	
$1g_{9/2}2d_{5/2}$	−0.90	0.34	0.13	0.04	0.10
$(1g_{9/2})^2$	−0.79	0.24	0.39	−0.01	0.15
$1h_{9/2}2f_{7/2}$	−0.50	−0.19	0.35	−0.08	0.18
$1h_{9/2}1i_{13/2}$	−0.70	−0.20	0.64	−0.10	0.41

[a] These were extracted from the data using Eq. (II.3). Only the first four coefficients are given. For $j_1=j_2$ multiplets, the higher coefficients were constrained to zero.

$$V_{\mathrm{CEN}} = U_{\mathrm{W}}(r) + U_{\mathrm{M}}(r)P^r + U_{\mathrm{B}}(r)P^\sigma + U_{\mathrm{H}}(r)P^rP^\sigma , \tag{III.3}$$

where P^r and P^σ are the space and spin exchange operators.

Another representation is the spin–isospin representation with

$$V_{\mathrm{CEN}} = U_0(r) + U_\sigma(r)\vec{\sigma}_1\cdot\vec{\sigma}_2 + U_\tau(r)\vec{\tau}_1\cdot\vec{\tau}_2 + U_{\sigma\tau}(r)(\vec{\sigma}_1\cdot\vec{\sigma}_2)(\vec{\tau}_1\cdot\vec{\tau}_2) . \tag{III.4}$$

The third representation, the triplet–singlet even-odd representation, is given by

$$V_{\mathrm{CEN}} = U_{\mathrm{SO}}(r)P^{\mathrm{SO}} + U_{\mathrm{SE}}(r)P^{\mathrm{SE}} + U_{\mathrm{TO}}(r)P^{\mathrm{TO}} + U_{\mathrm{TE}}(r)P^{\mathrm{TE}} , \tag{III.5}$$

where P^{SO}, P^{SE}, P^{TO}, and P^{TE} are the singlet–odd, singlet–even, triplet–odd, and triplet–even projection operators, respectively.

In Eqs. (III.3)–(III.5) above, all the local potentials, $U_n(r)$, may have different radial dependences and strengths and their shapes may be more complicated than a single Yukawa or Gaussian form.

As the experimental data separates naturally into the $T=0$ and $T=1$ matrix elements, the triplet–singlet even–odd representation in Eq. (III.5) will be used in this paper. Only the singlet–even and triplet–odd components will contribute to the $T=1$ matrix elements, while only the singlet–odd and triplet–even components will contribute to the $T=0$ matrix elements. The radial dependence of all $U_n(r)$'s were taken to be sums of no more than two Yukawa shapes. Any spin dependence will be represented by the inequality between the appropriate singlet and triplet components.

Of the possible types of noncentral interactions, only two were considered here. They are the tensor interaction

$$V_{\mathrm{Tensor}} = U_{\mathrm{Tensor}}(r)\left[\frac{3(\vec{\sigma}_1\cdot\vec{r})(\vec{\sigma}_2\cdot\vec{r}) - r^2(\vec{\sigma}_1\cdot\vec{\sigma}_2)}{r^2}\right] \tag{III.6}$$

and the two-body spin–orbit interaction

$$V_{\mathrm{LS}} = U_{\mathrm{LS}}(r)\vec{L}\cdot\vec{S} , \tag{III.7}$$

where $S=\frac{1}{2}(\vec{\sigma}_1+\vec{\sigma}_2)$ and $\vec{L}$ is the relative orbital angular momentum between the two interacting nucleons. Both of these noncentral forces will act only in the spin–triplet state ($S=1$) and consequently only the odd components will contribute to the $T=1$ matrix elements, while only the even components will contribute to the $T=0$ matrix elements.

To demonstrate some of the features with a central interaction, Fig. 11 shows the $T=0$ and $T=1$ matrix elements for the $(1h_{9/2}2f_{7/2})$ and $(1h_{9/2}2f_{5/2})$ multiplets computed with a pure Wigner admixture ($U_{\mathrm{SO}} = U_{\mathrm{SE}} = U_{\mathrm{TO}} = U_{\mathrm{TE}}$) and a single Yukawa interaction having ranges of 0.1, 1.0, or 5.0 fm with $\nu = 0.1578$ fm^{-2}. For $T=0$, the matrix elements show a strong curvature for the shortest range which becomes less and less pronounced as the range becomes comparable to the size of the wave functions. The pattern is similar for the two multiplets, throughout. For the $T=1$ matrix elements, on the other hand, the pattern is very different for the two multiplets for a short-range interaction. The matrix element with the minimum J is largest (most negative) for the $1h_{9/2}2f_{5/2}$ multiplet, while the $1h_{9/2}2f_{7/2}$ matrix element is largest for the maximum

TABLE X. Multipole coefficients for $T=1$ (MeV). [a]

Multiplet	$\gamma_{0,1}$	$\gamma_{1,1}$	$\gamma_{2,1}$	$\gamma_{3,1}$	$\gamma_{4,1}$
$1p_{3/2}1d_{5/2}$	−0.03	1.20	−0.33	0.12	
$1d_{3/2}1f_{7/2}$	0.32	0.04	−0.53	−0.12	
$1g_{9/2}1d_{5/2}$	0.14	0.17	−0.19	−0.01	−0.02
$1h_{9/2}2f_{7/2}$	0.056	−0.051	−0.062	−0.027	−0.046
$1h_{9/2}1i_{13/2}$	0.043	−0.022	−0.085	−0.026	−0.060

[a] These were extracted from the data using Eq. (II.3). Only the first four coefficients are given.

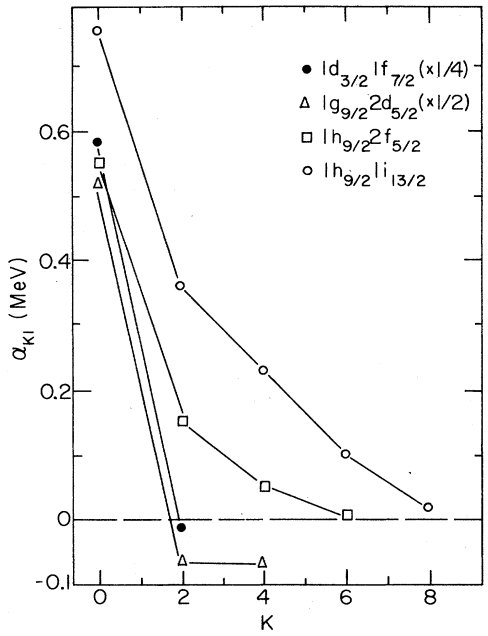

FIG. 10. Even isovector multipole coefficients for the $j_1 \neq j_2$ data.

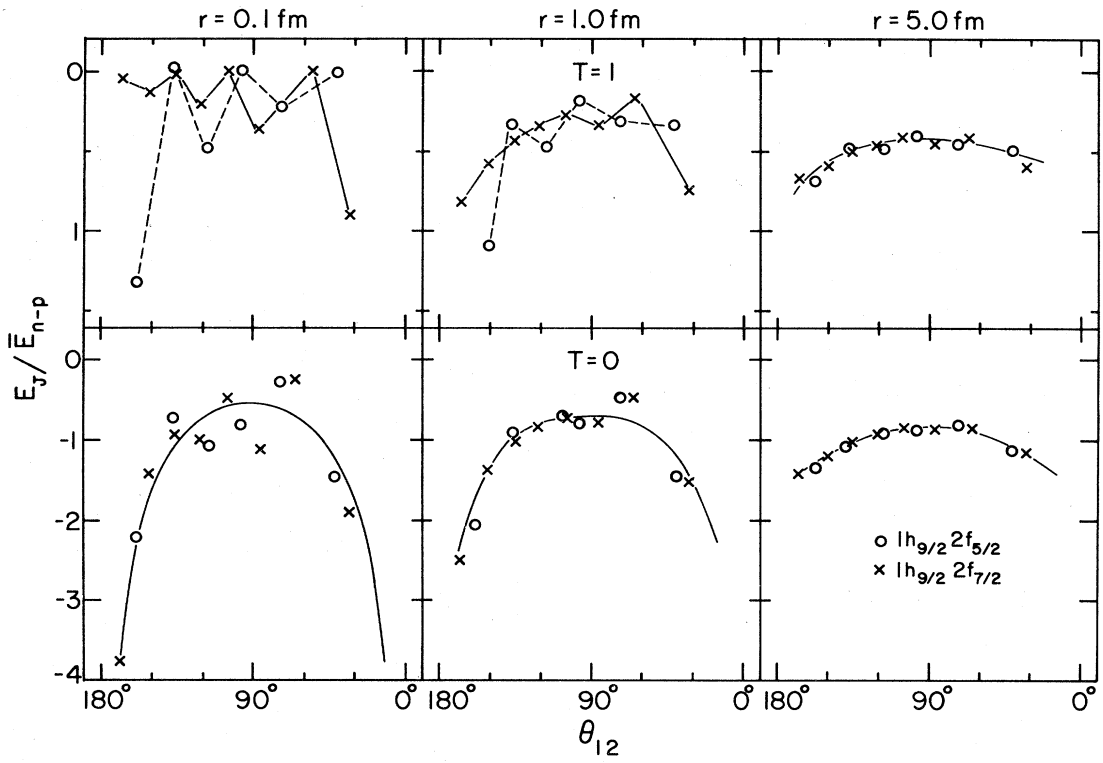

FIG. 11. Calculated $T=0$ and $T=1$ matrix elements for the $(1h_{9/2}2f_{7/2})$ and $(1h_{9/2}2f_{5/2})$ multiplets with various range Yukawa potentials and a Wigner interaction ($V_{\text{singlet}}=V_{\text{triplet}}$, $V_{\text{even}}=V_{\text{odd}}$). The lines are used to emphasize the trends in the matrix elements.

J. This lopsided behavior is still present with 1 fm range in the interaction but has disappeared for 5 fm. For this long range the matrix elements vary only slightly with J, this variation is very similar in the two multiplets, and the matrix elements are also nearly the same in the two isospin states.

The difference in the two multiplets is also shown in Fig. 12, where $(E_J^{\text{singlet}}-E_J^{\text{triplet}})/(E_J^{\text{singlet}}+E_J^{\text{triplet}})$ is plotted for $r=1.0$ fm. In other words, this is the pattern of the matrix elements for the spin-dependent part of the interaction, and the pattern depends on whether $j_1=l_1\pm\frac{1}{2}$ and $j_2=l_2\pm\frac{1}{2}$ or $j_1=l_1\pm\frac{1}{2}$, and $j_2=l_2\mp\frac{1}{2}$.

An alternative way of expressing these patterns is in terms of multipole coefficients, as is done in Fig. 13. Here we see that the even coefficients decrease with increasing K. As the range becomes larger the higher multipole coefficients decrease compared to the monopole. The odd coefficients show a similar decrease with the sign depending on the relative spin orientations in the two orbits, and the decrease in magnitude with increasing K is less pronounced.

Another feature is shown in Table XI. For the short-range interaction the even components of the force dominate. For a medium range (1.0 fm) interaction, the triplet–odd matrix elements become larger but the singlet–odd is still small compared to triplet–even. Only at 5 fm does the singlet–odd become appreciable. For a delta function force the odd part of the interaction has no contribution; for long-range the even and odd contributions become equal and the singlet–triplet ratio is 1:3.

Finally the pattern of matrix elements for the $1h_{9/2}2f_{5/2}$ and $1h_{9/2}2f_{7/2}$ multiplets with noncentral interactions is shown in Fig. 14. It is clear that the tensor interaction can fit features of the data that the other components cannot fit well; it can change the pattern of low-J matrix elements more than that for states with higher J. Whether the LS interactions can fit data not

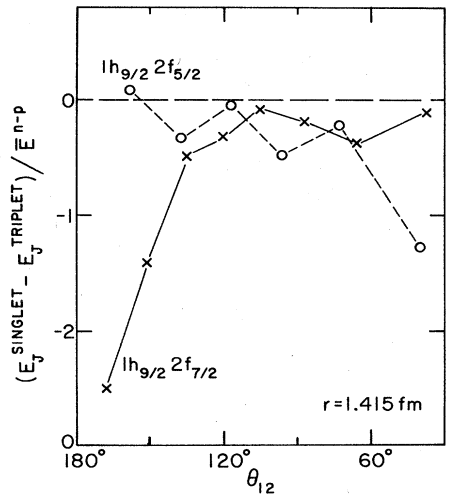

FIG. 12. The difference between calculated singlet and triplet matrix elements (isospin averaged) for the $(1h_{9/2}2f_{7/2})$ and $(1h_{9/2}2f_{5/2})$ multiplets, emphasizing the sensitivity of the $j=l+s$ and $j=l-s$ nature of the orbits to any spin dependence in the interaction.

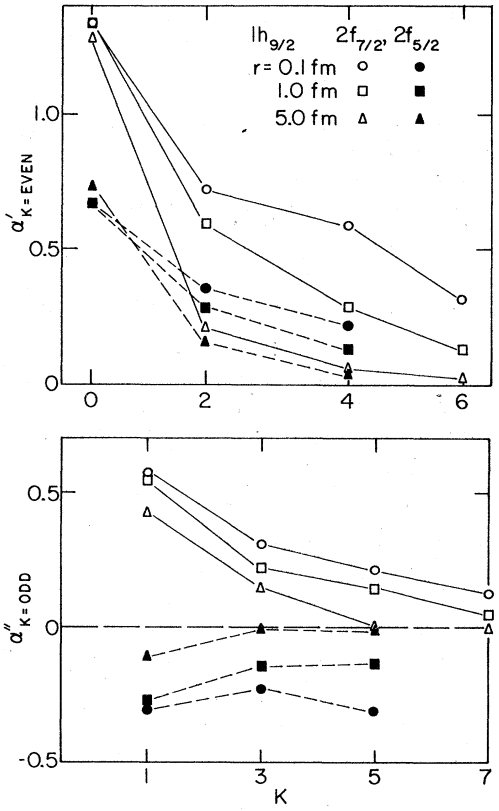

FIG. 13. Multipole coefficients for the $(1h_{9/2}2f_{7/2})$ and $(1h_{9/2}2f_{5/2})$ multiplets. The even coefficients are $\alpha'_K \equiv \alpha_{K,n-p}/\bar{\alpha}_{0,n-p}$ where $2\bar{\alpha}_0 \equiv \alpha_0(1h_{9/2}2f_{7/2}) + \alpha_0(1h_{9/2}2f_{5/2})$. The odd coefficients are for $\alpha''_K \equiv (\alpha_{K,\text{singlet}} - \alpha_{K,\text{triplet}})/2\bar{\alpha}$; $\alpha_{K,\text{singlet}} = \alpha_{K,\text{triplet}}$ for odd K with a Wigner force. In both cases, the rate of decrease in the coefficients with increasing K changes with the range of the interaction.

fit by other terms in the interaction is not clear from the qualitative features.

B. Calculation of the matrix elements

The calculation of the two-body matrix elements was done in a conventional manner. In the jj-coupling scheme, the $T=1$ matrix elements were required to be antisymmetric in space and spin, the $T=0$ matrix elements were required to be symmetric, while the neutron–proton matrix elements had no explicit symmetry.

TABLE XI. Relative average strength of matrix elements with a central force and no spin dependence (Wigner mixture). [a]

	$\bar{E}$ (%)			
	$T=0$		$T=1$	
Range (fm)	Singlet odd	Triplet even	Singlet even	Triplet odd
0.1	0	74	25	1
1.0	7	50	18	25
5.0	11	39	14	36

[a] The % contribution to $\bar{E}_{n-p}$ from the various components of the interaction are given. The values are for the $1h_{9/2}2f_{7/2}$ multiplet, but any large multiplet will give similar results.

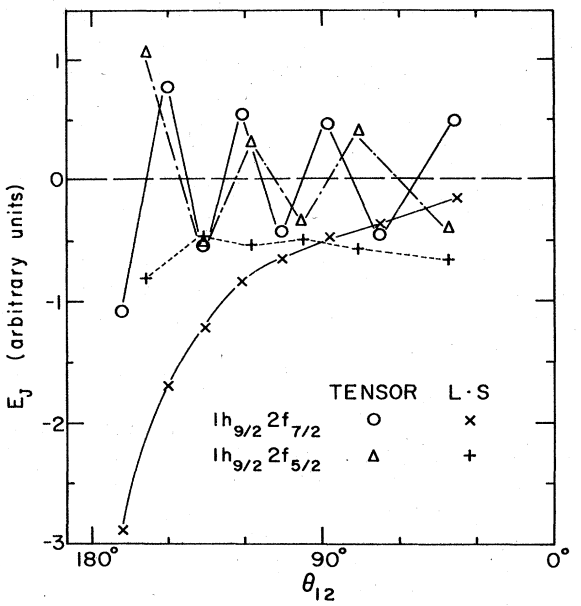

FIG. 14. Calculated matrix elements with noncentral forces.

First, the jj-matrix elements were transformed to the LS-coupling scheme and the corresponding LS matrix elements were then evaluated. These LS matrix elements were expanded in the usual manner in terms of Slater integrals and an angular matrix element involving Clebsch–Gordan and Racah coefficients (de-Shalit and Talmi, 1963).

The necessary Slater integrals were evaluated by using the Talmi coefficients and the Talmi integrals (Ford and Konopinski, 1958).

An alternative and equivalent method of evaluating the Slater integrals is to transform to the relative and center-of-mass coordinates using the Moshinsky brackets (Moshinsky, 1958; 1959; Brody and Moshinsky, 1960; Brody *et al.*, 1960). The matrix element in the relative coordinate system can then be evaluated and combined with the appropriate Moshinsky brackets to give the desired Slater integral. This alternative approach was used to evaluate the matrix elements of the two-body spin–orbit interaction given by Eq. III.7).

In all cases, the radial part of the single-particle wave function was assumed to have a harmonic oscillator shape. Harmonic-oscillator radial wave functions fall off more rapidly at large r than do, for example, radial wave functions in a Woods–Saxon well. For short-range potentials, this difference at large r is not important, as most of the contributions to the matrix elements for bound particles come from the interior region and it is believed that this choice of wave functions gives a fairly good estimate of the radial part of the matrix element (True *et al.*, 1971).

C. Weighting of the matrix elements in the fitting procedure

The choice of the relative weight factors had to be made with some caution. The point is that substantial differences in magnitude exist among the matrix elements, as seen in Figs. 8 and 9, for instance. The en-

ergies get smaller rapidly with increasing atomic weight. There is also a substantial difference between the $T=0$ and $T=1$ matrix elements, particularly around ^{208}Pb. While the $T=0$ and $T=1$ data could be fit independently, since in the representation used six terms in the interaction contribute only to $T=0$ and six to $T=1$, the n–p matrix elements force a correlation. It would also have been meaningless to assign weights in the usual fashion from experimental errors, since these play a relatively minor role in the true uncertainties. As another extreme it would have been equally meaningless to weight each matrix element by its size ($W_i \propto 1/E_i$), since this would have required that values of E_i that are zero or near zero be fit exactly no matter what happens otherwise.

The procedure adopted was to take the average absolute value of the matrix elements $\langle|E|\rangle_{\mathrm{Av}}$ for each $(j_1 j_2)_T$ multiplet, in order to avoid difficulties in cases where $\langle E_i\rangle_{\mathrm{Av}}$ was near zero, and use $W_i \approx (\langle|E_i|\rangle_{\mathrm{Av}})^{-1}$. The weights W_i were reduced below this value for matrix elements that were judged to be less well determined than others. The weights were also reduced for n–p multiplets to minimize the influence that the large $T=0$ contributions would have on the components of the $T=1$ interaction. The values of the weights used are given in Table XII.

The total contribution to χ^2 of the $T=0$ and $T=1$ matrix elements should thus be roughly the same for the same level of fit in the relative magnitudes of matrix elements. The contribution to χ^2 from the n–p data should be smaller. To repeat, the increased weight given to the $T=1$ matrix elements is not an expression of their greater accuracy, but is a device to allow them to balance the influence of the much larger $T=0$ matrix elements which would dominate even the $T=1$ terms in the interaction by way of the correlation introduced in fitting the n–p data.

TABLE XII. Oscillator constants and assignment of weights for the least-squares procedure. Unless otherwise indicated, the same weighting W_i was used for both the $T=0$ and $T=1$ matrix elements.

Configuration		ν (fm^{-2})	W_i	Level of confidence [a]
$(1p_{3/2})^2$, $(1p_{3/2}1p_{1/2})$	$T=0,1$	0.37	0.1	0.3
$(1d_{5/2})^2$	$T=0,1$	0.293	0.2 [b]	0.4
$(1d_{5/2}1p_{3/2})$	$T=0,1$	0.293	0.05	0.01
$(1d_{3/2})^2$	$T=0,1$		0.3	0.6
	$T=0$	0.283	0.2	0.4
$(1d_{3/2}1f_{7/2})$	$T=1$	0.283	0.6	0.3
$(1f_{7/2})^2$	$T=0$		0.3	0.5
	$T=1$	0.245	0.5	0.5
$(1f_{7/2}2p_{3/2})$	n–p	0.245	0.2	0.1
$(1g_{9/2})^2$	$T=0$		0.6	0.5
	$T=1$	0.213	3.0	1.0
	$T=0$	0.213	0.9	0.75
$(1g_{9/2}2d_{5/2})$	$T=1$	0.213	3.0	0.75
$(1h_{9/2}1i_{13/2})$, $(1h_{9/2}2f_{7/2})$	$T=0$		1.4	1.0
	$T=1$		7.0 [c]	1.0
$(1h_{9/2}j)$	n–p	0.1578	1.4	0.3
$(3p_{1/2}j)$	n–p	0.1578	0.1	0.03
$(1h_{9/2})^2$, $(2g_{9/2})^2$	$T=1$	0.1578	1.0 [d]	0.3

[a] This reflects the factor by which the $1/\langle|E|\rangle_{\mathrm{av}}$ was multiplied to get W_i. It represents the subjective component in assigning weights in the least-squares fitting procedure.
[b] $W_i=0.1$ for the 0^+ and 4^+ matrix elements.
[c] $W_i=3.5$ for the 2^-, 3^-, 5^-, 1^+, and 2^+ matrix elements.
[d] $W_i=0.3$ for the 0^+ matrix elements.

D. The need for various components in the interaction

The apparent need for two ranges in the $T=1$ matrix elements has been discussed earlier. To explore this need as well as the need for noncentral forces systematically, the least-squares procedures were carried out first with only one term in the interaction for each isospin, finding the ones that gave the lowest χ^2, then introducing a second term finding the one that improved χ^2 most, etc., until all 12 components were included. A typical set of results from such calculations is given in Table XIII for $r_1=1.415$ and $r_2=2.0$ fm.

The combination of two ranges listed in the table needs some explanation. It was found, not unexpectedly, that the strength of the two components V_1 and V_2 corresponding to Yukawa potentials with ranges r_1 and r_2, were strongly correlated. That is to say, the values of V_1 and V_2 fluctuate rather strongly with relatively minor changes in the other constraints. Possibly a more useful way of stating the results is in a combination of the parameters where this correlation is removed. This was approximately accomplished by defining

$$U_A \equiv V_A \frac{e^{-x_1}}{x_1}$$
$$U_B \equiv V_B\left[\frac{e^{-x_1}}{x_1} - \alpha^{-1}\frac{e^{-x_2}}{x_2}\right], \tag{III.8}$$

where α is calculated in such a way that the average matrix element of U_B over all the states calculated here is zero ($\overline{E}^{(B)}=0$). In other words $\alpha \equiv \sum\epsilon^{(2)}/\sum\epsilon^{(1)}$, where $\epsilon^{(1)}$ and $\epsilon^{(2)}$ are the matrix elements calculated with unit strength of V_1 and V_2, and the sum is over all states. Of course, $U_{\mathrm{TOTAL}}=U_1+U_2=U_A+U_B$. V_1 and V_2 are then related to V_A and V_B by

$$V_A = V_1 + \alpha V_2, \quad V_B = -\alpha V_2 \tag{III.9}$$

and inversely

$$V_1 = V_A + V_B, \quad V_2 = -V_B/\alpha.$$

The errors expressed for V_A and V_B are more nearly independent, while the errors in V_1 and V_2 tend to be strongly correlated.

Several features should be noted in Table XIII. For the $T=0$ data, the triplet-even interaction alone accomplishes most of the fit, almost entirely from a single range. The remaining components of the interaction improve the fit only slightly [the tensor-even part of the interaction helps primarily with the low-J matrix elements, as expected from Fig. 14, e.g., the 0^- member of the $(1h_{9/2}2g_{9/2})$ multiplet, noted by Kim and Rasmussen (1963)]. A second range did not improve matters much.

For the $T=1$ fit, on the other hand, a second compo-

TABLE XIII. Results of least squares fitting with constraints for $r_1 = 1.415$ fm and $r_2 = 2.0$ fm. V (MeV).

Constraints on $T=0$ only [a]						
S. O.$_A$	S. O.$_B$ [b]	Tr. E.$_A$	Tr. E.$_B$ [b]	Tens. E.	LS. E.	χ^2 [c]
						10.3(18.8, 22.4) [d]
		−57				1.19(1.27, 2.82)
17.6		−59				1.15(1.20, 2.91)
		−58		−34		1.08(1.12, 1.42)
17.7		−59		−34		1.04(1.06, 1.33)
3.7	122	−55	−63	−43	−0.4	1.00(1.00, 1.00)
Constraints on $T=1$ only [a]						
S. E.$_A$	S. E.$_B$	Tr. O.$_A$	Tr. O.$_B$	Tens. O.	LS. O.	χ^2 [c]
						5.2(9.7, 1.44) [d]
		5.4				5.0(9.2, 1.31)
−15.5		10.2				3.5(6.3, 1.19)
−1.6	−197	5.8				2.4(3.9, 1.08)
−18.8		19.3	−194			1.41(1.84, 1.35)
−12.0	−88	15.8	−162			1.24(1.47, 1.30)
−13.6	−70	16.5	−163		2.7	1.10(1.19, 1.45)
−13.5	−36	15.2	−171	−6.1	3.4	1.00(1.00, 1.00)
Constraints on non-central forces [e]						
S. E.$_A$	S. E.$_B$	S. O.$_A$	S. O.$_B$	Tr. E.$_A$	Tr. E.$_B$	Tr. O.$_A$	Tr. O.$_B$	χ^2
−12.0	−88.9			−57		15.9	−161	1.42(1.27, 1.47, 3.25)
−12.0	−88.6	16.3		−59		15.9	−161	1.40(1.19, 1.47, 3.5)
−12.0	−88.9	10.1	62.7	−58	−12.1	15.9	−161	1.39(1.19, 1.47, 3.5)
−11.7	−65	3.1	126	−56	−58	14.8	−168	1.18(0.93, 1.37, 1.00)

[a] The remaining interactions, relevant to the other isospin, were allowed to vary. They changed only minimally.

[b] The V_A, V_B parameterization used in the table is defined in terms of V_1 and V_2 in Eq. (III.9). The values of α were 2.75, 2.30, 2.32, 2.76 for the singlet–odd, triplet–even, singlet–even and triplet–odd interactions, respectively.

[c] χ^2 is normalized to 1.0 for the 12-parameter fit, the values in parentheses are the partial χ^2 for the isospin in question, and the n–p data normalized in the same way. For absolute values of χ^2 see Fig. 15.

[d] All terms in the interaction with the relevant isospin kept at zero. This χ^2 gives the scale of the size of the matrix elements.

[e] Both tensor and LS interactions constrained to zero, except for the last line, where the LS interaction only was kept at zero and the tensor force became −41.4 and −4.5 MeV for the even and odd components. The values in parentheses are the partial χ^2 for $T=0$, $T=1$, and n–p data.

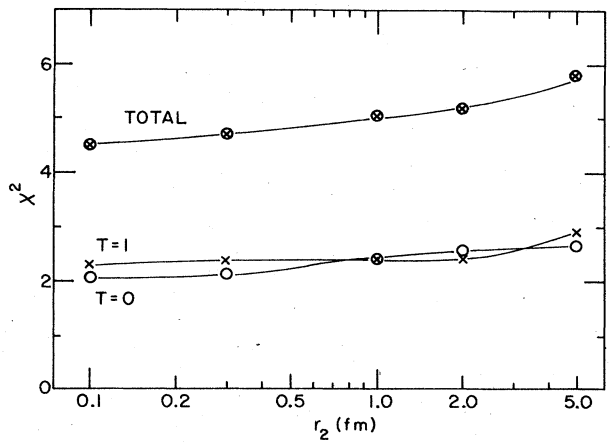

FIG. 15. Values of χ^2 for full 12-parameter fits as a function of the second Yukawa range (r_2) of the central interaction, with $r_1 = 1.415$ fm. The absolute scale of χ^2 is not meaningful because of the weights used. The relative contributions for $T=0$ and $T=1$ are correctly shown; the n–p contribution to χ^2 is about 0.2 on this scale.

nent is crucial in the triplet–odd interaction. A second component helps somewhat in the singlet interaction (~20% in χ^2) and the inclusion of the LS interaction improves χ^2 ~10%. The odd tensor force improves the level of the fit another 7%.

The pattern is generally similar for other choices of r_2, except that for $T=0$ the improvement for a second range becomes noticeable for small values of r_2.

E. Search on the range of interactions

As has already been stated, the interactions were always composed of Yukawa shapes. For each term of the central interaction, one of the Yukawa components was fixed at the one-pion exchange range ($r_1 = 1.415$ fm), as was the single component for the tensor and spin–orbit terms. The value of χ^2 as a function of the range of the second component in the interaction is shown in Fig. 15. We see that the curve is rather flat and perhaps a small ($r_2 \approx 0.1$ fm) value of r_2 is preferred, primarily by the $T=0$ matrix elements. But any $r_2 \lesssim 2.0$ fm is about equally good. One should note, as was stated above,

TABLE XIV. Parameters of the central [a] interaction in MeV [b] with various choices of r_2. [c]

r_2 (fm)	S. E.$_A$	S. E.$_B$	S. O.$_A$	S. O.$_B$	Tr. E.$_A$	Tr. E.$_B$	Tr. O.$_A$	Tr. O.$_B$	χ^2 [d]
0.1	−14.3	11.8 (0.611×10^{-3})	3.2	−31.6 (0.143×10^{-4})	−55.1	27.6 (0.692×10^{-3})	15.0	33.5 (0.143×10^{-4})	4.93
0.3	−14.1	13.3 (1.54×10^{-2})	3.7	−35.2 (2.70×10^{-3})	−55.2	30.0 (1.69×10^{-7})	14.8	39.5 (2.71×10^{-3})	5.03
1.0	−13.5	41.0 (0.415)	3.9	−116 (0.325)	−55.3	76.4 (0.421)	14.7	150.7 (0.325)	5.08
2.0	−13.5	−36 (2.32)	3.7	122 (2.75)	−55.5	−62.6 (2.30)	15.2	−171 (2.76)	5.05
5.0	−14.3	−9.7 (165.7)	7.4	29.9 (244)	−56.4	−14.5 (161.6)	16.1	−61.9 (250)	5.51

[a] The tensor and LS interactions were also varied but remained reasonably constant at -42 ± 3 and -5 ± 1 MeV for the even and odd tensor components and -0.7 ± 0.3 and 3.3 ± 0.6 MeV for the LS interaction.

[b] The value of r_1 was fixed at 1.415 fm.

[c] The values of α, allowing conversion to the V_1–V_2 parameterization by Eq. (III.9), are given in parentheses under the V_B values.

[d] Values of χ^2 for all the data. The absolute scale is meaningless because of the weighting factors.

that a second range is only mildly required for $T=0$, but for $T=1$ there is a singularity in χ^2 for $r_2=r_1$ not shown in Fig. 15.

A delta function interaction ($r_2=0$) clearly would not fit the $T=1$ data since the matrix elements of the odd-state interaction become identically zero. This was already clear from Table XI; one may note this trend in the values of α for the even and odd interactions in Table XIV. For $r_2\lesssim1.0$ fm the values of α are nearly the same, for $r_2=0.3$ fm $\alpha_{even}/\alpha_{odd}\approx5$, while it becomes ≈40 for $r_2=0.1$ fm. This reflects the enormous values of V_2 ($\approx10^6$ MeV) for this range.

The strengths for the various choices of r_2 are given in Table XIV. We see, as expected, that the values of V_A are quite constant while the values of V_B vary somewhat. The sign of V_B changes depending on whether $r_2>r_1$ or $r_2<r_1$. There is not very much difference as a function of r_2, nor did it make much difference when r_1 was fixed at a value other than 1.415 fm.

In Figs. 16 and 17 the various interactions corresponding to some of the entries in Table XIV are plotted. For the triplet–odd interaction, where the need for a second range is best defined, it is clear that the various combinations are, in fact, rather similar with an attractive core and a repulsive long-range component, the two roughly cancelling in the volume integrals. $U(r)r^2$ is plotted to make this feature clear. For the singlet–even interaction the same feature is seen, though not quite so clearly, while for the $T=0$ components, the second range is barely needed and the shape is not well defined.

F. Errors and recommended values

As has already been mentioned, the errors are best expressed in terms of V_A and V_B. One such case is given in Table XV. The errors correspond to the arbitrary

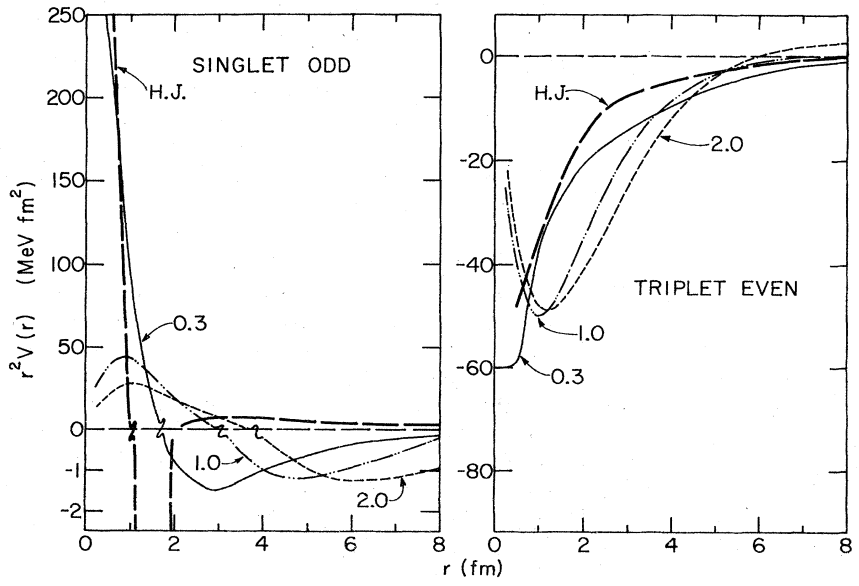

FIG. 16. Plot of the central components of the interaction for $T=0$, with various choices of the range for the second Yukawa (r_2). The curve labeled H.J. is the Hamada-Johnson interaction (without the hard core). Note that $r^2U(r)$ is plotted, not $U(r)$, to emphasize the contributions to the volume integrals (and approximately the matrix elements) from different regions of r.

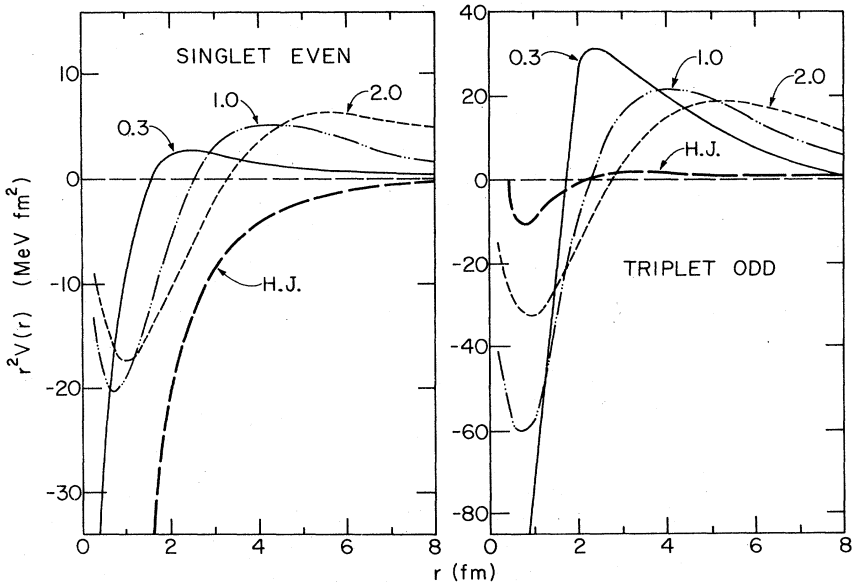

FIG. 17. Plot of the central components of the interaction for $T=1$, with various choices of the range for the second Yukawa (r_2). The curve labeled H.J. is the Hamada-Johnson interaction (without the hard core). Note that $r^2U(r)$ is plotted, not $U(r)$.

choice of a change of 1% in χ^2. Correlations tend to be small ($\lesssim 0.5$). Similar errors are obtained for the various constraints and the other choices of ranges.

What choice of interaction to take as "best" is a matter of taste and convenience. In many cases, the slight improvements obtained by inclusion of the noncentral components of the interaction may not be worthwhile. In Table XVI therefore the parameters for two choices of r_2 are given without the noncentral components. For an even simpler form, with only five parameters in the central interaction, one should consult the first line under noncentral constraints in Table XIII; this gives a total χ^2 of 8.9, to be compared to the other two values in Table XVI.

One should note that these relatively small changes in χ^2 are not very significant. The calculated matrix elements with a full 12-parameter fit for $r_2=2.0$ fm, as given in the appropriate lines of Table XIII and in Table XVII, are shown along with the data in Figs. 4–7 and in the Appendix. The calculated matrix elements using only the five parameters of the central interaction are also shown for some cases in Figs. 4 and 6. The 32% deterioration in χ^2 is not apparent on visual inspection. The fit with $r_2=2.0$ fm is used since the fits with small r_2, though marginally better in χ^2, result in absurdly high values of V_2.

G. Shell-model calculations

Standard shell-model calculations have been done on several nuclei in the lead region using some of the interactions obtained in Sec. III.E. The first set is that with $r_2=2.0$ fm, as given in Table XVII, except that the spin-orbit force was assumed to be equal to zero. The second set was for $r_2=0.1$ fm, as given in Table XVI, with the same tensor force as the first set, and again no spin–orbit force.

As has been seen in Table XIV and Fig. 15, χ^2 varied slowly as the second range r_2 was changed with the shorter ranges being slightly preferred; this preference came entirely from the $T=0$ matrix elements. As was seen in Fig. 4 and in the Appendix, the $j_1=j_2$, $J=0$, $T=1$ matrix elements tend to be fit well; the measured matrix elements tend to be larger than the calculated ones. A reasonable guess is that the configuration mixing introduced by pair correlations may be the source of this systematic trend.

Tables XVIII–XXI compare the results of shell-model calculations of the low-lying $T=1$ levels in ^{210}Pb and ^{206}Pb with the experimental values. In Tables XVIII and XX, one sees that the first interaction, with $r_2=2.0$ fm, causes very little configuration mixing for all levels. The second interaction, with smaller r_2, results in

TABLE XV. Typical errors in the interaction strengths in MeV with $r_1=1.415$ fm and $r_2=2.0$ fm for a 1% change in χ^2.

$T=0$ S. O.$_A$	S. O.$_B$	Tr. E.$_A$	Tr. E.$_B$	Tens. E.	LS. E.
3.7 ± 9	122 ± 73	−56 ± 2	−63 ± 20	−43 ± 10	−0.4 ± 2
$T=1$ S. E.$_A$	S. E.$_B$	Tr. O.$_A$	Tr. O.$_B$	Tens. O.	LS. O.
−13.5 ± 1.2	−36 ± 13	15.2 ± 1.1	−171 ± 12	−6.1 ± 1.4	3.4 ± 0.8

TABLE XVI. Some values of interaction potentials in MeV using only central interactions.

r_2	S. E.$_A$	S. E.$_B$	S. O.$_A$	S. O.$_B$	Tr. E.$_A$	Tr. E.$_B$	Tr. O.$_A$	Tr. O.$_B$	χ^2
2.0	−12.0	−88.9	10.1	62.7	−58.2	−12.1	15.9	−161	7.04
0.3	−14.8	22.0	6.9	−25.2	−56.4	18.4	16.4	39.2	6.79
0.1	−15.0	18.6	6.0	−23.8	−56.1	18.3	16.5	33.4	6.63
r_2	S. E.$_1$	S. E.$_2$	S. O.$_1$	S. O.$_2$	Tr. E.$_1$	Tr. E.$_2$	Tr. O.$_1$	Tr. O.$_2$	χ^2
2.0	−100.85	38.36	72.82	−22.84	−70.30	5.27	−144.94	58.37	7.04
0.3	7.26	−1428	−18.33	9351	−38.04	−10.84	+55.61	−14470	6.79
0.1	3.65	−30 514	−17.74	1 661 151	−37.81	−26 503	49.91	−2 328 444	6.63

much more configuration mixing for the 0^+ levels. This, of course, is the well-known origin of a "pairing force" deduced as a consequence of an attractive short-range interaction. There is very little change for the higher spin levels. Not only does the shorter-range force have larger diagonal matrix elements (E_D in the tables) for the 0^+ levels, it causes more configuration mixing, resulting in better agreement with the experimental values than is the case when the first force is used. In fact, a value for r_2 of 0.1 fm may be too small and 0.2 or 0.3 fm would probably give better fits. The other levels are only slightly changed as r_2 is varied.

Tables XIX and XXI compare the squared amplitudes of the various components in the ground-state wave functions of ^{210}Pb and ^{206}Pb with experimentally measured values. These tables also indicate that the shorter range is definitely preferred for 0^+ ground states.

Shell-model calculations have also been done on the low-lying $T=1$ levels of ^{210}Po with both forces. In this case, the results show similar effects for the 0^+ ground states. All other higher states are very pure and there is very little difference in the matrix elements of the two forces.

It should be noted that the correlations for 0^+ states tend to favor a short range for the $T=1$ interaction. The slight improvement in χ^2 for small r_2 that is noted in Fig. 15 was due entirely to the $T=0$ data, and primarily the triplet–even component. There is no data where off-diagonal $T=0$ matrix elements may be tested; shell-model calculations for the mixed isospin ^{210}Bi case are consistent with the data.

IV. DISCUSSION

A. Other attempts to fit matrix elements

There has been considerable success in fitting nuclear data with shell-model calculations that assume a delta function (or surface delta) interaction (Glaudemans *et al.*, 1967). When more than n–p data are involved, it has often been found necessary to use a "delta function plus isospin-dependent monopole" interaction. These results are qualitatively consistent with the findings described here, in that two interaction ranges are required, especially in $T=1$.

A more extensive attempt, covering most of the data described here, has been published by Molinari *et al.* (1975). Semiclassical expressions were used for the matrix elements and coefficients for a "delta function plus monopole, plus dipole, plus quadrupole" force were obtained. These coefficients were determined independently for at least eight groupings of the data, depending on T, on whether $j_1=j_2$, and on whether j_1+j_2+J is even or odd for $j_1\neq j_2$. All in all, not counting those coefficients which failed to significantly improve the fit and were thus left at zero, four coefficients were needed to fit the $j_1=j_2$ data for the $E_J/\overline{E}$ values, and four more for the $j_1\neq j_2$ n–p data. When the $j_1\neq j_2$ data (not including the $1g_{9/2}2d_{5/2}$ multiplet) were considered separately by isospin, seven coefficients were needed. The values of $\overline{E}$ were not fit. Altogether, if only the separate isospin data are considered, eleven independent parameters were obtained to fit a substantial subset of the data considered here. Perhaps the principal conclusion regarding the relation of this work to ours is that a simple "delta function plus quadrupole" interaction is inadequate, that substantial monopole components are required, and that the parameterization of the data separately by the types of orbits replaces the spin and isospin dependent interactions of our work.

Another attempt at fitting matrix elements with an effective interaction is that of Mairle and Wagner (1972). He used experimental matrix elements applying somewhat different criteria from those used here and using data from transfer reactions in the s–d shell. The values of the matrix elements used are similar to the values adopted here, though significant differences exist in some of the selections of what to include. All the data were fit by a single-range effective interaction and only the relative magni-

TABLE XVII. Parameters in MeV for the 12-parameter fit with $r_1=1.415$ fm and $r_2=2.0$ fm.

S. E.$_A$	S. E.$_B$	S. O.$_A$	S. O.$_B$	Tr. E.$_A$	Tr. E.$_B$	Tr. O.$_A$	Tr. O.$_B$	Tens. E.	Tens. O.	LS. E.	LS. O.
−13.5	−35.8	3.7	122	−55.5	−62.6	15.2	−171	−42.52	−6.10	−0.43	3.42
S. E.$_1$	S. E.$_2$	S. O.$_1$	S. O.$_2$	Tr. E.$_1$	Tr. E.$_2$	Tr. O.$_1$	Tr. O.$_2$	Tens. E.	Tens. O.	LS. E.	LS. O.
−49.32	15.47	125.53	−44.37	−118.09	27.27	−155.82	62.06	−42.52	−6.10	−0.43	3.42

TABLE XVIII. Comparison of "effective" matrix elements in ^{210}Pb from a shell-model calculation. |Amp.| is the absolute value of the amplitude of the given configuration after diagonalization. E_D is the diagonal matrix element and E_M is the energy eigenvalue after diagonalization. Force 1 and Force 2 correspond to two choices of the second range in the interaction as described in the text. The experimental values are taken from Table VIII.

		Force 1 (r_2=2.0 fm)			Force 2 (r_2=0.1 fm)			
Configuration	J^π	|Amp.|	E_D	E_M	|Amp.|	E_D	E_M	E_{exp}
$2g_{9/2}^2$	0_1^+	0.973	−0.527	−0.644	0.886	−0.932	−1.369	−1.244
	2_1^+	0.995	−0.120	−0.142	0.990	−0.259	−0.300	−0.449
	4_1^+	0.998	0.010	0.001	0.997	−0.069	−0.083	−0.153
	6_1^+	0.998	0.057	0.049	0.998	−0.003	−0.012	−0.050
	8_1^+	0.998	0.116	0.109	0.998	0.082	0.074	0.029

tude of the various components of the central interaction were varied. The fit was made multiplet by multiplet, as well as for all the data put together. The level of fit in the latter case is significantly worse than the level of fit in the present work.

A natural, more limited, extension of the present interaction is to the coupling of nucleons in Nilsson orbits in odd–odd (or even–even) deformed nuclei. The information available from such nuclei is, of course, very limited because in each case there are only two possible couplings yielding two matrix elements. For the odd–odd nuclei these are of the n–p mixed isospin type and thus do not add much information. They are quite well fit even by a delta-function interaction (Jones *et al.*, 1971). In the even–even case, the meaning of the absolute energies is somewhat dubious because of uncertainties due to blocking by two identical nucleons. The splitting has been looked at and appears to be consistent with the interaction proposed here (Katori and Weller, 1972; Weller, 1973).

A more general area of possible future investigations may be in the transitional region, where the quasiparticle model has had considerable success. One may well imagine in the Sn isotopes, for instance, where a particular neutron orbit is gradually filled as neutrons are being added, that multiplets based on the corresponding quasiparticle state will gradually change from the particle–particle to particle–hole types. This will cause a given multiplet to change from the inverted U shape to an upright U shape, with the multiplet essentially degenerate when the orbit is half filled (U_j^2=0.5). To our knowledge no such data are presently available.

B. Other properties of two-nucleon states

1. Magnetic moments

Recent years have allowed measurements of magnetic moments in several two-nucleon spectra. This permits an independent test of the purity of the wavefunction whatever the effective moment of the one-particle state, it should be reflected in the magnetic moments of the two-particle spectra. When both orbits are the same (j_1=j_2) this means that the two-particle states should have the same g-factors as the one-particle state. If core-polarization effects were to change, this would lead to inconsistencies in the g factors.

In A=42 the g factor of the 6^+ state in ^{42}Ca is −0.415 ± 0.015[4] and it is −0.456 for the ^{41}Ca ground state (Young *et al.*, 1975). The purity of the $(1f_{7/2})^2$ states was discussed in Sec. II.A.6; some admixtures do exist in A=42. In ^{90}Nb the g factors for the 6^+ and 8^+ states are 0.620 ± 0.004 and 0.6176 ± 0.0005, respectively (Holland *et al.*, 1975; Hagn *et al.*, 1974); these are remarkably consistent and support the purity of these configurations. In recent work Faestermann (1974) and Baba *et al.* (1973) find the g factor of the $8^+, 1h_{9/2}^2$ state in ^{210}Po to be 0.912 ± 0.011, and that of the 6^+ state to be the same within one percent; the ^{209}Bi ground state has g=0.910. In ^{210}Bi Faestermann finds the 5^- and 7^- members of the $1h_{9/2}2g_{9/2}$ multiplet to have g=0.309 ± 0.007 and 0.304 ± 0.006, respectively. For ^{40}K two magnetic moments are known, belonging to the 3^- and 4^- members of the $(\nu 1f_{7/2}\pi 1d_{3/2}^{-1})$ multiplet. The magnetic moments of ^{41}Ca and ^{39}K ground states may be used to compute the expected g factors. The values are −0.43 ± 0.03 (−0.456) for the 3^- state and −0.3245 ± 0.0001 (−0.3123) for the 4^- ground state; the values in parentheses are the predicted ones (Brandolini *et al.*, 1974). This latter case was already interpreted in a very similar context by de-Shalit (1961). All available magnetic-moment data thus support the results derived from transfer reactions regarding the purity of the two-particle spectra. It is beyond the scope of this paper to attempt the calculation of the g factors for the various single-particle states.

2. Gamma-ray transition probabilities

A question to be mentioned is the electromagnetic transition rates between members of two-particle multiplets. Within a multiplet M1 transitions will tend to predominate; between multiplets this is not necessarily the case. Absolute transition probabilities with a few percent accuracy are generally difficult to come by, but even when such data are available they are subject to a number of uncertainties in interpretation. Competing electric and magnetic transitions, varying effective charges and moments, and small admixtures from nearby collective excitations that may alter transition probabilities by disproportionate amounts, all introduce large uncertainties. No attempt is made here to review the state of knowledge for such transitions.

[4]This result is inconsistent with the value of g=−0.50 ± 0.03 of Nomura *et al.* (1971).

TABLE XIX. Comparison of the calculated squared amplitudes of the various configurations in the ground state of ^{210}Pb with the experimental values. Force 1 and Force 2 are described in the text, and the experimental values are taken from Igo (1971).

	Configuration						
	$2g^2_{9/2}$	$1i^2_{11/2}$	$1j^2_{15/2}$	$3d^2_{5/2}$	$4s^2_{1/2}$	$2g^2_{7/2}$	$3d^2_{3/2}$
Experiment	0.67	0.16	0.17	0.01	0.0015	0.015	0.0035
Force 1 (r_2=2.0 fm)	0.947	0.015	0.024	0.007	0.001	0.004	0.001
Force 2 (r_2=0.1 fm)	0.784	0.088	0.078	0.025	0.004	0.015	0.005

C. Conclusion

A reasonably satisfactory over-all fit is obtained to well over one hundred experimental matrix elements from nuclei throughout the periodic table. The interaction has 12 parameters, though all but the last 32% in χ^2 is accomplished by only five parameters in the central interaction. The need for a two-range interaction, with a shorter range attraction and a longer range repulsion is necessary for $T=1$. There is little sensitivity to the exact range; the change in sign of the potential occurs at 2–3 fm, as may be seen in Fig. 17. For the $T=0$ interaction the need for a second range is much less clear. The tensor term in the interaction improves the fit for a few specific matrix elements, while the L-S term seems to improve the level of fit in a more general way. All in all, the noncentral terms in the interaction account for a ~30% improvement in χ^2.

A comparison of the present interaction with the interaction between free nucleons (Hamada and Johnston, 1962) was shown in Figs. 16 and 17. The $T=0$ parts of the interaction are reasonably similar in magnitude and shape, but the $T=1$ part is quite different. A comparison of various free nucleon–nucleon interactions (Moravcsik, 1972) shows some fluctuations in the detailed shapes, but none approach the present result for the $T=1$ interactions.

An attempt has been made by Elliott (1968) to extract matrix elements of the nucleon-nucleon interaction directly from the phase shifts without the intervention of a potential. These so-called Sussex matrix elements have been used in shell-model calculations but it is not clear how a meaningful comparison could be made between this work and the present one.

Of all the possible matrix elements between valence nucleons which can occur throughout the periodic table, this investigation has only considered diagonal matrix elements; there is not enough reliable data available from transfer reactions to extract off-diagonal ones. We have not made use of the diagonal and off-diagonal matrix elements obtained by least-squares fit to experimental energy level data (the third approach in Sec. I) except for those of Cohen and Kurath (1965). Not all possible diagonal matrix elements were considered because, in many cases, the configurations are strongly mixed with other configurations and the data from reactions are not sufficient to sort out admixtures uniquely. For example, the $3p^2_{1/2}$, $3p^2_{3/2}$, and $2f^2_{5/2}$ configurations in the lead region are strongly mixed and it is at present not possible to experimentally resolve the appropriate matrix elements except for 0^+ ground states. One can hope that if a single residual interaction is a valid concept, then this interaction should also be applicable to those diagonal and off-diagonal matrix elements where considerable configuration mixing occurs. The shell-model calculations described in Sec. III.G offer some encouragement in this direction.

Golin and Zamick (Golin *et al.*, 1974; Golin and Zamick, 1975) have used a previous version of our interaction to calculate the dipole giant resonance, the energy of the isobaric analog resonance, and the change in single-particle energy spacings in the f–p shell as the $1f_{7/2}$

TABLE XX. Comparison of "effective" matrix elements in ^{206}Pb from a shell-model calculation. |Amp.| is the absolute value of the amplitude of the given configuration after diagonalization where 1.000^- means a number slightly less than 1.0. E_D is the diagonal matrix element, and E_M is the energy eigenvalue after diagonalization. Force 1 and Force 2 are described in the text, and the experimental values were deduced from Manthuruthil *et al.* (1972).

		Force 1 (r_2=2.0 fm)			Force 2 (r_2=0.1 fm)			
Configuration	J^π	|Amp.|	E_D	E_M	|Amp.|	E_D	E_M	E_{exp}
$3p^2_{1/2}$	0^+_1	0.963	−0.218	−0.304	0.851	−0.385	−0.696	−0.640
$3p_{1/2}2f_{5/2}$	2^+_1	0.933	−0.034	−0.105	0.948	−0.075	−0.144	−0.407
	3^+_1	0.999	0.111	0.108	0.999	0.101	0.099	0.130
$3p_{1/2}3p_{3/2}$	1^+_1	1.000^-	0.121	0.121	1.000^-	0.038	0.037	0.170
	2^+_2	0.941	−0.163	−0.180	0.940	−0.238	−0.289	−0.080
$2f^2_{5/2}$	0^+_2	0.942	−0.432	−0.497	0.808	−0.712	−0.827	−0.612
	2^+_3	0.972	−0.009	−0.014	0.944	−0.085	−0.088	0.008
	4^+_1	0.925	0.099	0.063	0.943	0.056	0.020	−0.096

TABLE XXI. Comparison of the calculated squared amplitudes of the various configurations in the ground state of ^{206}Pb with the experimental values. Force 1 and Force 2 are described in the text.

	Configuration					
	$3p^2_{1/2}$	$2f^2_{5/2}$	$3p^2_{3/2}$	$1i^2_{13/2}$	$2f^2_{7/2}$	$1h^2_{9/2}$
Experiment [a]	0.54	0.20	0.12	0.12	0.03	
Experiment [b]	0.65	0.25	0.20			
Force 1 (r_2=2.0 fm)	0.927	0.036	0.029	0.004	0.003	0.001
Force 2 (r_2=0.1 fm)	0.724	0.147	0.076	0.030	0.015	0.007

[a] Mukherjee and Cohen, 1962.
[b] Richard *et al.*, 1968.

shell is filled. Their conclusion is that an interaction of the present form comes much closer to fitting these quantities than more "realistic" (e.g., Kuo–Brown) interactions. It is the monopole part of the present interaction that plays the major role in these quantities. They have also suggested that the origin of the repulsive term in our interaction is due to the requirement of translational invariance, a constraint that need not be present for all core-polarization effects. Golin and Zamick (1975) use an interaction in which the long-range part is restricted to the $S=1$ (triplet) terms and the results are not seriously affected. This is consistent with the present result discussed in Sec. III.E; in Table XIII it was clear that the second range was most important in the triplet-odd interaction.

It thus may be hoped that the above interactions will be more generally useful in structure calculations. Similarly, it remains to be seen whether the present residual interaction will be useful when applied to reaction calculations.

An important question is the relation of the present empirical results to our theoretical understanding of an effective interaction. There is certainly little in the present theoretical perspective that would lead one to expect a single effective interaction to have general validity. The matrix elements from the free nucleon–nucleon interaction require substantial modification to fit the energy level data, as has been amply demonstrated by Kuo and Brown (1966), Herling and Kuo (1972), and others. Does the present result imply a theoretical simplification? Does nuclear matter behave as a dielectric medium, modifying the free nucleon–nucleon interaction in a uniform way? Or is the present pattern a more or less accidental consequence of more complicated aspects of the problem? The answers to these questions remain for the future.

ACKNOWLEDGMENTS

The work in this paper has received the benefit of discussions with many of our colleagues both at Argonne and elsewhere. Of special help however has been Dr. Dieter Kurath, who has provided critical comments and constructive insights and has helped to clarify many important points. The origins of this work owe much to the perspectives and influence of J. B. French. One of us (J.P.S.) is indebted to the Alexander von Humboldt Foundation for a U. S. Senior Scientist Award and to Professors P. Kienle, H.-J. Körner, and H. Mang of the Technical University of Munich for making it possible to complete an important portion of this work while on sabbatical leave. The assistance of N. Anantaraman and T. Renner at various stages of this work has been of considerable help.

APPENDIX

Table A.1 presents a list of particle–particle matrix elements in MeV determined from experimental data and values from fit.

TABLE A.1. The following is a list of particle–particle matrix elements in MeV determined from experimental data[a] and values from fit.[b]

Configuration	J	$E_{J,T=0}$		$E_{J,T=1}$		$E_{J,\text{n-p}}$
$(1p_{3/2})^2$ [c]	0			−3.2	−3.3	
	1	−3.6	−4.2			
	2			−0.2	−1.1	
	3	−7.2	−7.1			
$1p_{1/2}1p_{3/2}$ [c]	1	−6.2	−9.0	+0.9	−0.6	
	2	−4.0	−8.8	−1.0	−1.6	
$(1d_{5/2})^2$	0			−3.2	−2.3	
	1	−3.3	−2.2			
	2			−0.9	−0.7	
	3	−1.6	−1.8			
	4			0.3	0.1	
	5	−3.7	−4.0			

TABLE A.1 *(Continued)*

Configuration	J	$E_{J,T=0}$		$E_{J,T=1}$		$E_{J,\text{n-p}}$	
$1p_{3/2}1d_{5/2}$ [d]	1	0.4	−2.1	−2.6	−2.2		
	2	−2.0	−3.5	−0.9	0.0		
	3	−1.0	−0.5	0.2	−0.8		
	4	−7.1	−7.9	1.2	0.9		
$(1d_{3/2})^2$	0			−2.9	−2.0		
	1	−2.2	−1.5				
	2			0.2	−0.4		
	3	−2.7	−2.8				
$1d_{3/2}1f_{7/2}$	2	−3.0	−5.1	−0.4	−0.4		
	3	−1.7	−2.8	0.3	−0.2		
	4	−1.6	−1.4	1.1	0.3		
	5	−2.1	−3.5	0.0	−0.5		
$(1f_{7/2})^2$	0			−2.13	−1.78		
	1	−2.11	−1.45				
	2			−0.81	−0.51		
	3	−1.04	−0.93				
	4			0.06	0.0		
	5	−0.87	−1.09				
	6			0.28	0.24		
	7	−2.28	−2.65				
$1f_{7/2}2p_{3/2}$ [c]	2					−0.64	−0.84
	3					−0.57	−0.60
	4					−0.14	−0.12
	5					−0.90	−1.15
$(1g_{9/2})^2$	0			−1.84	−1.58		
	1	−1.32	−1.14				
	2			−0.67	−0.44		
	3	−0.63	−0.54				
	4			−0.04	−0.01		
	5	−0.44	−0.53				
	6			0.16	0.14		
	7	−0.59	−0.73				
	8			0.23	0.28		
	9	−1.49	−1.91				
$1g_{9/2}2d_{5/2}$	2	−0.56	−0.92	−0.54	−0.58		
	3	−0.69	−0.75	−0.08	0.07		
	4	−0.40	−0.29	0.0	0.06		
	5	−0.96	−0.81	0.34	0.27		
	6	−0.79	−0.25	0.41	0.29		
	7	−1.46	−1.87	0.17	0.33		
$1h_{9/2}3p_{1/2}$ [d]	4					−0.079	−0.100
	5					−0.142	−0.194
$1h_{9/2}3p_{3/2}$ [c]	3					−0.304	−0.332
	4					−0.119	−0.098
	5					−0.100	−0.044
	6					−0.222	−0.205
$1h_{9/2}2f_{5/2}$ [c]	2					−0.264	−0.380
	3					−0.063	−0.122
	4					−0.060	−0.072
	5					−0.140	−0.142
	6					−0.043	−0.020
	7					−0.291	−0.436

TABLE A.1 *(Continued)*

Configuration	J	$E_{J,T=0}$		$E_{J,T=1}$		$E_{J,\text{n-p}}$	
$1h_{9/2}2f_{7/2}$	1	−1.308	−1.420	−0.032	−0.028		
	2	−0.955	−0.843	0.097	−0.003		
	3	−0.536	−0.561	0.120	0.147		
	4	−0.520	−0.486	0.100	0.078		
	5	−0.359	−0.313	0.127	0.149		
	6	−0.416	−0.423	0.048	0.052		
	7	−0.278	−0.190	0.162	0.161		
	8	−0.565	−0.637	−0.115	−0.076		
$1h_{9/2}1i_{13/2}$	2	−2.944	−2.312	−0.182	−0.221		
	3	−1.452	−1.215	−0.002	−0.072		
	4	−0.809	−0.827	0.075	0.119		
	5	−0.660	−0.768	0.036	0.056		
	6	−0.433	−0.454	0.140	0.124		
	7	−0.494	−0.642	0.036	0.044		
	8	−0.322	−0.287	0.162	0.130		
	9	−0.577	−0.682	0.019	−0.001		
	10	−0.305	−0.211	0.201	0.195		
	11	−1.190	−1.207	−0.166	−0.202		
$1h_{9/2}2g_{9/2}$ [c]	0					−0.606	−0.739
	1					−0.653	−0.665
	2					−0.333	−0.363
	3					−0.306	−0.268
	4					−0.152	−0.141
	5					−0.220	−0.175
	6					−0.106	−0.058
	7					−0.220	−0.180
	8					−0.027	0.002
	9					−0.375	−0.363
$3p_{1/2}2f_{5/2}$ [d]	2					−0.144	−0.208
	3					−0.199	−0.336
$3p_{1/2}2f_{7/2}$ [d]	3					−0.239	−0.330
	4					−0.140	−0.243
$3p_{1/2}1i_{13/2}$ [d]	6					−0.153	−0.168
	7					−0.110	−0.090
$(1h_{9/2})^2$ [c]	0			−1.44	−0.84		
	2			−0.22	−0.17		
	4			0.05	−0.01		
	6			0.10	0.04		
	8			0.18	0.12		
$(2g_{9/2})^2$ [c]	0			−1.24	−0.58		
	2			−0.449	−0.113		
	4			−0.153	0.038		
	6			−0.050	0.091		
	8			0.029	0.154		
Total number of matrix elements		60		50		32	

[a] These numbers are the ones discussed in Sec. II.A. The first entry in this table is the experimental value.

[b] The second entry in this table is the calculated value of the matrix element with the 12-parameter fit values given in Table XVII with $r_1 = 1.415$ fm and $r_2 = 2.0$ fm. These calculated values are plotted in Figs. 4–6.

[c] These data were included in the fitting procedure with significantly reduced weight ("level of confidence" $\lesssim 0.3$).

[d] These data were effectively excluded from the fitting procedure ("level of confidence" $\lesssim 0.1$).

REFERENCES

Ajzenberg-Selove, F., 1972, Nucl. Phys. A **190**, 1.
Alford, W. P., J. P. Schiffer, and J. J. Schwartz, 1968, Phys. Rev. Lett. **21**, 156.
Alford, W. P., J. P. Schiffer, and J. J. Schwartz, 1971, Phys. Rev. C **3**, 860.
Anantaraman, N., and J. P. Schiffer, 1972, Phys. Lett. B **37**, 229.
Arima, A., S. Cohen, R. D. Lawson, and M. H. Macfarlane, 1968, Nucl. Phys. A **108**, 94.
Baba, C. V. K., D. B. Fossan, T. Faestermann, F. Feilitzsch, P. Kienle, and C. Signorini, 1973, Phys. Lett. B **43**, 483.
Ball, J. B., and M. R. Cates, 1967, Phys. Lett. B **25**, 126.
Barrett, B. R., and M. R. Kirson, 1970, Nucl. Phys. A **148**, 145.
Barrett, B. R., 1975, ed., *Effective Interactions and Operators in Nuclei* (Proceedings of the Tucson International Topical Conference on Nuclear Physics, University of Arizona, Tucson, 2–6 June 1975) (Springer-Verlag, Berlin), Lecture Notes in Physics, Vol. **40**.
Bearse, R. C., J. R. Comfort, J. P. Schiffer, M. M. Stautberg, and J. C. Stoltzfus, 1969, Phys. Rev. Lett. **23**, 864.
Betts, R. R., C. Gaarde, O. Hansen, J. S. Larsen, and S. Y. van der Wert, Kernfysisch Versneller Instituut, Groningen, Annual Report, 1974.
Bhatia, T. S., W. W. Daehnick, and T. R. Canada, 1971, Phys. Rev. C **3**, 1361.
Bjerregaard, J. H., O. Hansen, O. Nathan, L. Vistisen, R. Chapman, and S. Hinds, 1968, Nucl. Phys. A **113**, 484.
Bohr, A., 1968, in *Proceedings of the International Symposium on Nuclear Structure, Dubna* (International Atomic Energy Agency, Vienna), p. 179.
Bohr, A., and B. R. Mottelson, 1969, in *Nuclear Structure* (Benjamin, New York), Vol. I, p. 69.
Brandolini, F., C. Rossi Alvarez, and G. B. Vingiani, 1974, Phys. Lett. B **49**, 261.
Brody, T. A., and M. Moshinsky, 1960, *Tables of Transformation Brackets for Nuclear Shell-Model Calculations* (Gordon and Breach, New York).
Brody, T. A., G. Jacob, and M. Moshinsky, 1960, Nucl. Phys. **17**, 16.
Cline, C. K., W. P. Alford, H. E. Gove, and R. Tickle, 1972, Nucl. Phys. A **186**, 273.
Cline, D., M. J. A. De Voigt, P. B. Vold, O. Hansen, O. Nathan, and D. Sinclair, 1974, Nucl. Phys. A **233**, 91.
Cohen, S., and D. Kurath, 1965, Nucl. Phys. **73**, 1.
Cohen, S., R. D. Lawson, M. H. Macfarlane, S. P. Pandya, and M. Soya, 1967, Phys. Rev. **160**, 903.
Comfort, J. R., J. V. Maher, G. C. Morrison, and J. P. Schiffer, 1970, Phys. Rev. Lett. **25**, 383.
Comfort, J. R., and J. P. Schiffer, 1971, Phys. Rev. C **4**, 803.
Courtney, W. J., and H. T. Fortune, 1972, Phys. Lett. B **41**, 4.
Crawley, G. M., E. Kashy, W. Lanford, and H. G. Blosser, 1973, Phys. Rev. C **8**, 2477.
Crozier, D. J., 1972, Nucl. Phys. A **198**, 209.
de-Shalit, A., 1961, Nucl. Phys. **22**, 677.
de-Shalit, A., and I. Talmi, 1963, in *Nuclear Shell Theory* (Academic, New York), p. 208.
Elliott, J. P., A. D. Jackson, H. A. Mavromatis, E. A. Sanderson, and B. Singh, 1968, Nucl. Phys. A **121**, 241.
Endt, P. M., and C. Van der Leun, 1973, Nucl. Phys. A **214**, 1.
Erskine, J. R., 1964, Phys. Rev. **135**, B110.
Erskine, J. R., 1966, Phys. Rev. **149**, 854.
Erskine, J. R., W. W. Buechner, and H. A. Enge, 1962, Phys. Rev. **128**, 720.
Erskine, J. R., D. J. Crozier, J. P. Schiffer, and W. P. Alford, 1971, Phys. Rev. C **3**, 1976.
Faestermann, T., 1974, Ph.D. thesis, Technical University of Munich, W. Germany.
Fann, H., J. P. Schiffer, and U. Strohbusch, 1973, Phys. Lett. B **44**, 19.
Fant, B., 1971, Phys. Scr. **4**, 175.
Fink, C. L., and J. P. Schiffer, 1974, Nucl. Phys. A **225**, 93.
Ford, K. W., and E. J. Konopinski, 1958, Nucl. Phys. **9**, 218.
Forster, J. S., K. Bearpark, J. L. Hutton, and J. F. Sharpey-Schafer, 1970, Nucl. Phys. A **150**, 30.
Glaudemans, P. W. M., P. J. Brussaard, and B. H. Wildenthal, 1967, Nucl. Phys. A **102**, 593.
Goldstein, S., and I. Talmi, 1956, Phys. Rev. **102**, 589.
Goldstein, S. and I. Talmi, 1957, Phys. Rev. **103**, 718.
Golin, M., R. W. Sharp, and L. Zamick, 1974, Nucl. Phys. A **221**, 546.
Golin, M., and L. Zamick, 1975, Nucl. Phys. A **251**, 129.
Goode, P., 1974, Phys. Lett. B **51**, 429.
Goode, P., and D. S. Koltun, 1972, Phys. Lett. B **39**, 159.
Hagn, E., P. Kienle, and G. Eska, 1974, in *Proceedings of the International Conference on Nuclear Structure and Spectroscopy*, edited by H. P. Blok and A. E. L. Dieperink (Amsterdam), Vol. 2, 576.
Hamada, T., and I. D. Johnston, 1962, Nucl. Phys. **34**, 382.
Hansen, O., J. R. Lien, O. Nathan, A. Sperduto, and P. O. Tjom, 1975, Nucl. Phys. A **243**, 100.
Harvey, T. F., and D. M. Clement, 1971, Nucl. Phys. A **176**, 592.
Herling, G. H., and T. T. S. Kuo, 1972, Nucl. Phys. A **181**, 113.
Heusler, A., and P. von Brentano, 1973, Ann. Phys. (N.Y.) **75**, 381.
Holland, R. E., F. J. Lynch, R. J. Mitchell, T. V. Ragland, and R. P. Scharenberg, 1975, Phys. Lett. B **58**, 43.
Igo, G., E. R. Flynn, B. J. Dropesky, and P. D. Barnes, 1971, Phys. Rev. C **3**, 349.
Jones, H. D., N. Onishi, T. Hess, and R. K. Sheline, 1971, Phys. Rev. C **3**, 529.
Katori, K., and F. Weller, 1972 (private communication).
Kim, Y. E., and J. O. Rasmussen, 1963, Nucl. Phys. **47**, 184.
Kim, Y. E., and J. O. Rasmussen, 1964, Phys. Rev. **135B**, B44.
Ko, C. M., T. T. S. Kuo, and J. B. McGrory, 1973, Phys. Rev. C **8**, 2379.
Kocher, D. C., and D. J. Horen, 1972, Nucl. Data B **7**, 299.
Koltun, D. S., 1973, Annu. Rev. Nucl. Sci. **23**, 163.
Kroon, J., B. Hird, and G. C. Ball, 1973, Nucl. Phys. A **204**, 609.
Kuo, T. T. S., 1968, Nuc. Phys. A **122**, 325.
Kuo, T. T. S., 1974, Annu. Rev. Nucl. Sci. **24**, 101.
Kuo, T. T. S., and G. E. Brown, 1966, Nucl. Phys. **85**, 40.
Kuo, T. T. S., and G. E. Brown, 1968, Nucl. Phys. A **114**, 241.
Kuo, T. T. S., and G. H. Herling, 1971, Naval Research Laboratory Memorandum Report 2258 (unpublished).
Lanford, W. A., W. P. Alford, and H. W. Fulbright, 1971, University of Rochester, Nuclear Structure Research Laboratory, Report UR-NSRL-44, 1971 (unpublished) and Bull. Am. Phys. Soc. **16**, 493.
Lawson, R. D., 1971, in Rutherford Centennial Symposium, Christchurch, New Zealand, July 7, 1971, p. 222.
Lewis, M. B., 1971, Nucl. Data B **5**, 631.
Li, T. K., D. Dehnhard, R. E. Brown, and P. J. Ellis, to be published (1975).
Ma, C. W., and W. W. True, 1973, Phys. Rev. C **8**, 2313.
Macfarlane, M. H., 1969, *Reaction Matrix in Nuclear Shell Theory*, Proceedings of the International School of Physics "Enrico Fermi," Course XL (Academic, New York).
Macfarlane, M. H., and J. B. French, 1960, Rev. Mod. Phys. **32**, 567.
Mairle, G., 1972, Habilitation thesis, Max-Planck-Institute for Nuclear Physics, Heidelberg (MPI H-1972-V28) unpub-

lished.
Mairle, G. and G. T. Wagner 1974, Phys. Lett. B **50**, 252.
Manthuruthil, J. C., D. C. Camp, A. V. Ramayya, J. H. Hamilton, J. J. Pinajian, and J. W. Doornebas, 1972, Phys. Rev. C **6**, 1870.
McCrory, J. B., B. H. Wildenthal, and E. C. Halbert, 1970, Phys. Rev. C **2**, 186.
Medsker, L. R., 1972, Nucl. Data B **8**, 599.
Meshkov, S. and C. W. Ufford, 1956, Phys. Rev. **101**, 734.
Moinester, M., J. P. Schiffer, and W. P. Alford, 1969, Phys. Rev. **179**, 984.
Molinari, A., M. B. Johnson, H. A. Bethe, and W. M. Alberico, 1975, Nucl. Phys. A **239**, 45.
Moravcsik, M. J., 1972, Rep. Prog. Phys. **35**, 587.
Moshinsky, M., 1958, Nucl. Phys. **8**, 19.
Moshinsky, M., 1959, Nucl. Phys. **13**, 104.
Motz, H. T., E. T. Jurney, E. B. Shera, and R. K. Sheline, 1971, Phys. Rev. Lett. **26**, 854.
Mukherjee, P., and B. L. Cohen, 1962, Phys. Rev. **127**, 1284.
Nathan, O., 1972, in *Proceedings of the International Symposium on Nuclear Structure,* Dubna, 1968 (International Atomic Energy Agency, Vienna), p. 191.
Nomura, T., T. Yamazaki, S. Nagamiya, and T. Katou, 1971, Phys. Rev. Lett. **27**, 523.
Ohnuma, H., J. R. Erskine, J. A. Nolen, Jr., J. P. Schiffer, and P. G. Roos, 1969, Phys. Rev. **177**, 1695.
Ohnuma, H., J. R. Erskine, J. P. Schiffer, J. A. Nolen, Jr., and N. Williams, 1970, Phys. Rev. C **1**, 496.
Osnes, E., and G. S. Warke, 1969, Phys. Lett. B **30**, 306.
Pandya, S. P., 1956, Phys. Rev. **103**, 956.
Polsky, L. M., C. H. Holbrow, and R. Middleton, 1969, Phys. Rev. **186**, 966.
Racah, G., 1942, Phys. Rev. **61**, 186.
Richard, P., N. Stein, C. D. Kavaloski, and J. S. Lilley, 1968, Phys. Rev. **171**, 1308.
Schiffer, J. P., 1969, in *Isospin in Nuclear Physics,* edited by D. H. Wilkinson (North-Holland, Amsterdam), Chap. 13, p. 665.
Schiffer, J. P., 1971a, Ann. Phys. (N.Y.) **66**, 798.
Schiffer, J. P., 1971b, in *Proceedings of the Topical Conference on the Structure of $1f_{7/2}$ Nuclei, Legnaro* (Padova), edited by R. A. Ricci (Editrice Compositori, Bologna), pp. 37–59.
Schiffer, J. P., 1972, in *The Two-Body Force in Nuclei,* edited by S. M. Austin and G. M. Crawley (Plenum, New York), p. 205.
Schiffer, J. P., 1975, in *Effective Interactions and Operators in Nuclei* (Proceedings of the Tucson International Topical Conference on Nuclear Physics, University of Arizona, Tucson, 2–6 June 1975), edited by B. R. Barrett (Springer-Verlag, Berlin), Lecture Notes in Physics **40**, p. 168.
Schwartz, J. J., D. Cline, H. E. Gove, R. S. Sherr, T. S. Bhatia, and R. H. Siemssen, 1967, Phys. Rev. Lett. **19**, 1482.
Serduke, F. J. D., D. Gloeckner, and R. D. Lawson (to be published, 1975).
Seth, K. K., J. A. Biggerstaff, P. D. Miller, and G. R. Satchler, 1967, Phys. Rev. **164**, 1450.
Sheline, R. K., C. Watson, and E. W. Hamburger, 1964, Phys. Lett. **8**, 121.
Talmi, I, 1957, Phys. Rev. **107**, 326.
Talmi, I., and R. Thieberger, 1956, Phys. Rev. **103**, 718.
Tickle, R., and J. Bardwick, 1971, Phys. Lett. B **36**, 32.
True, W. W., C. W. Ma, and W. T. Pinkston, 1971, Phys. Rev. C **3**, 2421.
Vary, J., and J. N. Ginocchio, 1971, Nucl. Phys. A **166**, 479.
Vold, P., D. Cline, J. J. A. deVoight, O. Hansen, and O. Nathan, University of Rochester, Nuclear Structure Research Laboratory 1974 Annual Report (unpublished).
Wagner, G. J., G. Mairle, U. Schmidt-Rohr, and P. Turek, 1969, Nucl. Phys. A **125**, 80.
Weller, F., 1973, Z. Phys. **262**, 425.
West, B. J., and D. S. Koltun, 1969, Phys. Rev. **187**, 1315.
Wiza, J. L., R. Middleton, and P. V. Hewka, 1966, Phys. Rev. **141**, 975.
Young, L. E., R. Breun, S. K. Bhattacherjee, D. B. Fossan, and G. D. Sprouse, 1975, Phys. Rev. Lett. **35**, 497.
Zisman, M. S., and B. G. Harvey, 1972, Phys. Rev. C **5**, 1031.